Article

Dietary salt promotes cognitive impairment through tau phosphorylation

https://doi.org/10.1038/s41586-019-1688-z

Received: 31 May 2018

Accepted: 24 September 2019

Published online: 23 October 2019

Giuseppe Faraco[1]*, Karin Hochrainer[1], Steven G. Segarra[1], Samantha Schaeffer[1], Monica M. Santisteban[1], Ajay Menon[1], Hong Jiang[2], David M. Holtzman[2], Josef Anrather[1] & Costantino Iadecola[1]*

Dietary habits and vascular risk factors promote both Alzheimer's disease and cognitive impairment caused by vascular factors[1–3]. Furthermore, accumulation of hyperphosphorylated tau, a microtubule-associated protein and a hallmark of Alzheimer's pathology[4], is also linked to vascular cognitive impairment[5,6]. In mice, a salt-rich diet leads to cognitive dysfunction associated with a nitric oxide deficit in cerebral endothelial cells and cerebral hypoperfusion[7]. Here we report that dietary salt induces hyperphosphorylation of tau followed by cognitive dysfunction in mice, and that these effects are prevented by restoring endothelial nitric oxide production. The nitric oxide deficiency reduces neuronal calpain nitrosylation and results in enzyme activation, which, in turn, leads to tau phosphorylation by activating cyclin-dependent kinase 5. Salt-induced cognitive impairment is not observed in tau-null mice or in mice treated with anti-tau antibodies, despite persistent cerebral hypoperfusion and neurovascular dysfunction. These findings identify a causal link between dietary salt, endothelial dysfunction and tau pathology, independent of haemodynamic insufficiency. Avoidance of excessive salt intake and maintenance of vascular health may help to stave off the vascular and neurodegenerative pathologies that underlie dementia in the elderly.

Vascular risk factors, including excessive salt consumption, have long been associated with cerebrovascular diseases and cognitive impairment[1–3]. A diet rich in salt is an independent risk factor for stroke and dementia[3,8–10] and has been linked to the cerebral small vessel disease that underlies vascular cognitive impairment[11], a condition that is associated with endothelial dysfunction and reduced cerebral blood flow (CBF)[12]. In mice, a high-salt diet (HSD) induces cognitive dysfunction by targeting the cerebral microvasculature through a gut-initiated adaptive immune response mediated by T_H17 lymphocytes[7]. The resulting increase in circulating IL-17 leads to inhibition of endothelial nitric oxide synthase (eNOS) and reduced vascular production of nitric oxide, which in turn impairs endothelial vasoactivity and lowers CBF by about 25%[7]. However, it remains unclear how hypoperfusion, resulting from an HSD or other vascular risk factors, leads to impaired cognition. The prevailing view is that hypoperfusion compromises the delivery of oxygen and glucose to energy-demanding brain regions that are involved in cognition[12,13]. However, the relatively small reduction in CBF that is associated with an HSD in mice[7] and vascular cognitive impairment in humans[14] may not be sufficient to impair cognitive function[15], suggesting that vascular factors beyond cerebral perfusion are involved.

Excessive phosphorylation of the microtubule-associated protein tau promotes the formation of insoluble tau aggregates, which are thought to mediate neuronal dysfunction and cognitive impairment in Alzheimer's disease and other tauopathies[16]. However, accumulation of tau has also been detected in cerebrovascular pathologies associated with endothelial dysfunction and cognitive impairment[5,6]. Therefore, we investigated whether tau accumulation rather than cerebral hypoperfusion contributes to the cognitive dysfunction induced by an HSD. First, we investigated whether an HSD induces phosphorylation of tau. Male C56Bl/6 mice were fed a normal diet or an HSD (4 or 8% NaCl—a commonly used model of excessive dietary salt corresponding to a 8–16-fold increase in salt content compared to regular mouse chow)[7,17]. Phosphorylation of tau epitopes that promote aggregation of tau and neuronal dysfunction[16] was assessed over time by western blotting. An HSD (8% NaCl) induced a sustained increase in phosphorylated tau (p-tau; detected using AT8 (pSer202 and pThr205) and RZ3 (pThr231) antibodies) in the neocortex and hippocampus without increasing total tau (detected using Tau 46; Fig. 1a). In the hippocampus, there was also an increase in tau phosphorylation measured using PHF13 and pSer199Ser202 antibodies (Extended Data Fig. 1a). AT8 tau phosphorylation was abolished by λ-protein phosphatase (Extended Data Fig. 1b). AT8 and RZ3 immunoreactivity were also increased in the neocortex of female mice fed an HSD (Extended Data Fig. 1c). The HSD did not increase acetylation of tau at K280, a post-translational modification that has been implicated in tau pathology[18] (Extended Data Fig. 1a). AT8 and MC1 immunoreactivity was detected in the piriform cortex, but we found no neurofibrillary tangles (Fig. 1b, Extended Data Fig. 1d, e). We found neither neuronal or white-matter damage, nor significant changes in astrocytes, microglia/macrophages or pericytes (Extended Data

[1]Feil Family Brain and Mind Research Institute, Weill Cornell Medicine, New York, NY, USA. [2]Department of Neurology, Hope Center for Neurological Disorders, Knight Alzheimer's Disease Research Center, Washington University, St. Louis, MO, USA. *e-mail: gif2004@med.cornell.edu; coi2001@med.cornell.edu

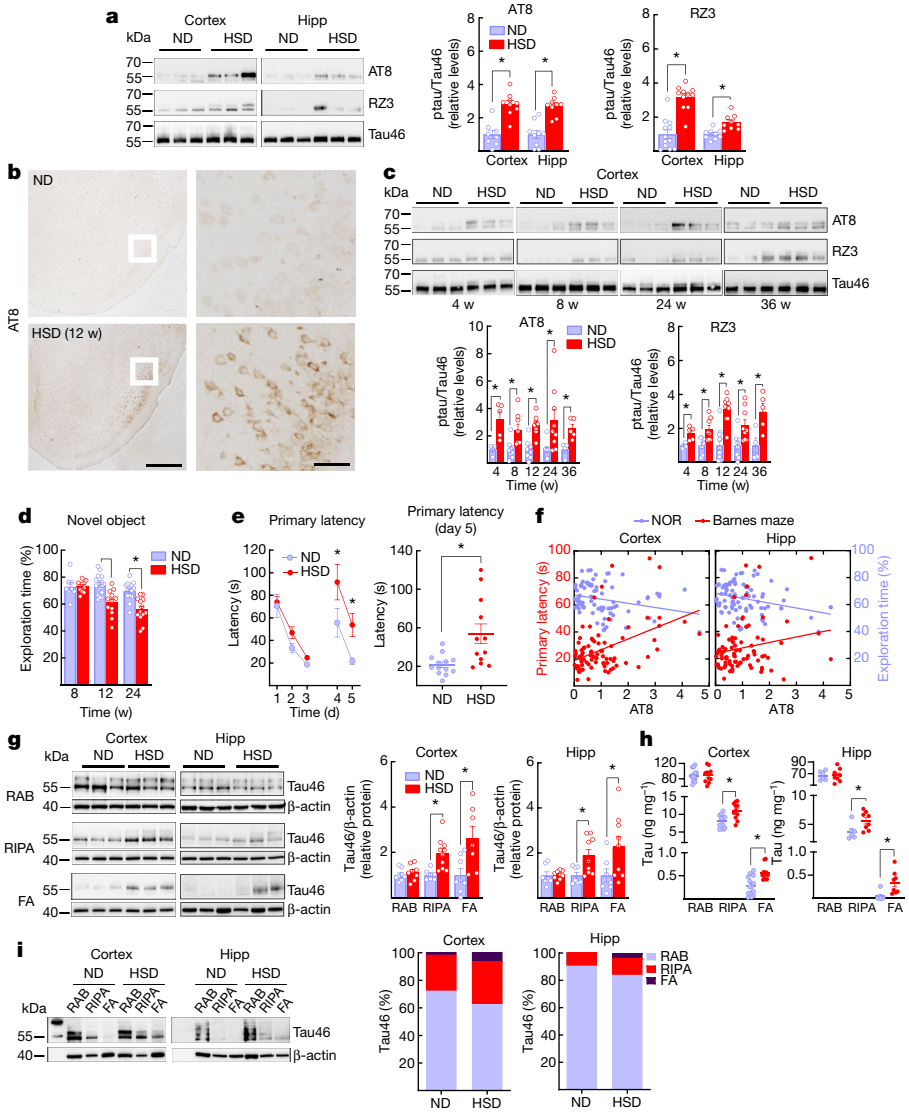

Fig. 1 | HSD increases tau phosphorylation and insoluble tau. a, HSD increases AT8 and RZ3 immunoreactivity (cortex: AT8, normal diet (ND)/HSD $n = 8/9$, $^*P < 0.0001$; RZ3, ND/HSD $n = 12/11$, $^*P < 0.0001$; hippocampus (Hipp): AT8, ND/HSD $n = 9/9$, $^*P < 0.0001$; RZ3, ND/HSD $n = 9/9$, $^*P = 0.0011$; two-tailed unpaired *t*-test for HSD versus ND). In all figures and legends, asterisks denote significant differences. **b**, HSD increases neuronal AT8 immunoreactivity in the piriform cortex. Right, magnified view of boxes on left (scale bars, 500 µm (left); 100 µm (right)). Representative images ($n = 5$ mice per group). **c**, Time course of neocortical increase in AT8 and RZ3. AT8, 4 weeks: ND/HSD $n = 4/5$, $^*P = 0.0116$; 8 weeks: ND/HSD $n = 9/8$, $^*P = 0.0066$; 24 weeks: ND/HSD $n = 8/9$, $^*P = 0.0152$; 36 weeks: ND/HSD $n = 4/5$, $^*P = 0.0087$; RZ3, 4 weeks: ND/HSD $n = 4/5$, $^*P = 0.0097$; 8 weeks: ND/HSD $n = 7/8$, $^*P = 0.0084$; 24 weeks: ND/HSD $n = 8/9$, $^*P = 0.0135$; 36 weeks: ND/HSD $n = 4/5$, $^*P = 0.0204$; two-tailed unpaired *t*-test for HSD versus ND. **d**, HSD induces deficits in recognition memory. Diet: $^*P < 0.0001$, time: $^*P = 0.0002$; 8 weeks: ND/HSD $n = 8/11$; 12 weeks: ND/HSD $n = 16/12$; 24 weeks: ND/HSD $n = 14/13$ mice per group, two-way ANOVA and Tukey's test. **e**, HSD induces deficits in spatial memory. Diet: $^*P = 0.0048$, time: $^*P < 0.0001$; ND/HSD $n = 13/12$, two-way repeated measures ANOVA and Bonferroni's test; primary latency day 5, ND/HSD $n = 13/12$, $^*P = 0.0031$ versus ND, two-tailed unpaired *t*-test. **f**, Neocortical and hippocampal levels of AT8 correlate with spatial learning impairment. AT8 cortex: Barnes maze $r = 0.4491$, $^*P < 0.0001$, $n = 84$; novel object recognition (NOR) $r = -0.2621$, $^*P = 0.0188$, $n = 80$; AT8 hippocampus: Barnes maze $r = 0.2073$, $^*P = 0.0462$, $n = 93$; NOR $r = -0.2915$, $^*P = 0.0053$, $n = 90$; Pearson's correlation coefficient. **g**, HSD increases levels of insoluble tau (western blotting) extracted in RIPA and FA fractions after 12 weeks. Cortex: RIPA, ND/HSD $n = 7/10$, $^*P = 0.0032$; FA, ND/HSD $n = 8/7$, $^*P = 0.0146$; hippocampus: RIPA, ND/HSD $n = 7/9$, $^*P = 0.0418$; FA, ND/HSD $n = 7/9$, $^*P = 0.0494$, two-tailed unpaired *t*-test for HSD versus ND. **h**, HSD increases levels of insoluble tau (electrochemiluminescence). Cortex: RIPA, ND/HSD $n = 11$, $^*P = 0.0050$; FA, ND/HSD $n = 14/11$, $^*P = 0.0028$; hippocampus: RIPA, ND/HSD $n = 6/8$, $^*P = 0.0380$; FA, ND/HSD $n = 7/8$, $^*P = 0.0037$; two-tailed unpaired *t*-test for HSD versus ND. **i**, HSD shifts tau from the RAB fraction to the less soluble RIPA and FA fractions. Cortex: ND/HSD $n = 9/8$, RAB, $P = 0.4234$, RIPA, $P = 0.5414$, FA, $^*P = 0.0325$; hippocampus: ND/HSD $n = 5/6$, RAB, $P = 0.2468$, RIPA, $P = 0.3290$, FA, $^*P = 0.0152$; two-tailed unpaired *t*-test for HSD versus ND. For gel source data see Supplementary Fig. 1. Data are expressed as mean ± s.e.m.

Fig. 2a–c). Increased AT8 immunoreactivity was also observed in the neocortex of mice fed with the 4% HSD (Extended Data Fig. 1f).

In the neocortex, AT8 immunoreactivity increased after 4 weeks and RZ3 immunoreactivity after 8 weeks of HSD, and both remained elevated for up to 36 weeks, whereas in the hippocampus AT8 immunoreactivity peaked at 12 and 36 weeks (Fig. 1c, Extended Data Fig. 1g). Starting after 12 weeks of HSD, mice exhibited difficulties in recognizing novel objects and developed a deficit in spatial memory for the Barnes maze (Fig. 1d, e, Extended Data Fig. 3a). Female mice fed an HSD also showed cognitive dysfunction (Extended Data Fig. 1c). The magnitude of phosphorylation at the AT8 and RZ3 epitopes was correlated with performance on the Barnes maze (Fig. 1f) and novel object recognition (Extended Data Fig. 3b). The HSD did not increase levels of amyloid-β ($A\beta_{38}$, $A\beta_{40}$ or $A\beta_{42}$) in the neocortex (Extended Data Fig. 3c). p-tau was also increased in

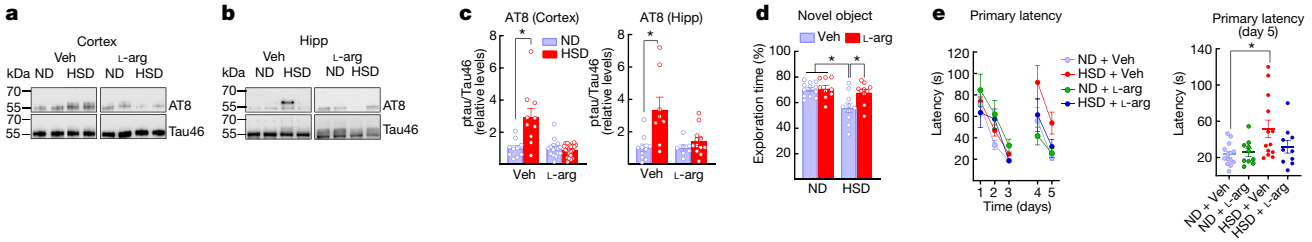

Fig. 2 | The NO precursor L-arginine prevents the increase in p-tau induced by HSD. a–**c**, Administration of L-arginine (10 g l^{-1} in drinking water), starting at week 8 of HSD and continued through week 12, suppresses AT8 accumulation in neocortex (**a**) and hippocampus (**b**); quantified in **c**. Cortex: vehicle (Veh), ND/HSD $n = 10/10$, L-arginine (L-arg), ND/HSD $n = 16/21$, $^*P = 0.0045$; hippocampus: Veh, ND/HSD $n = 10/8$, $^*P = 0.0067$, L-arg, ND/HSD $n = 7/12$, two-tailed unpaired *t*-test for HSD versus ND. **d**, **e**, L-Arginine treatment reduces the cognitive deficits induced by HSD in both the NOR test (Veh: ND/HSD $n = 12/10$; L-arg: ND/HSD $n = 6/11$; diet: $^*P = 0.0156$, treatment: $^*P = 0.0406$; two-way ANOVA and Tukey's test) and the Barnes maze (primary latency, diet: $^*P = 0.0182$, time: $^*P < 0.0001$, two-way repeated measures ANOVA and Tukey's test; primary latency day 5, $^*P = 0.0439$; Kruskal–Wallis test). For gel source data see Supplementary Fig. 1. Data are expressed as mean ± s.e.m.

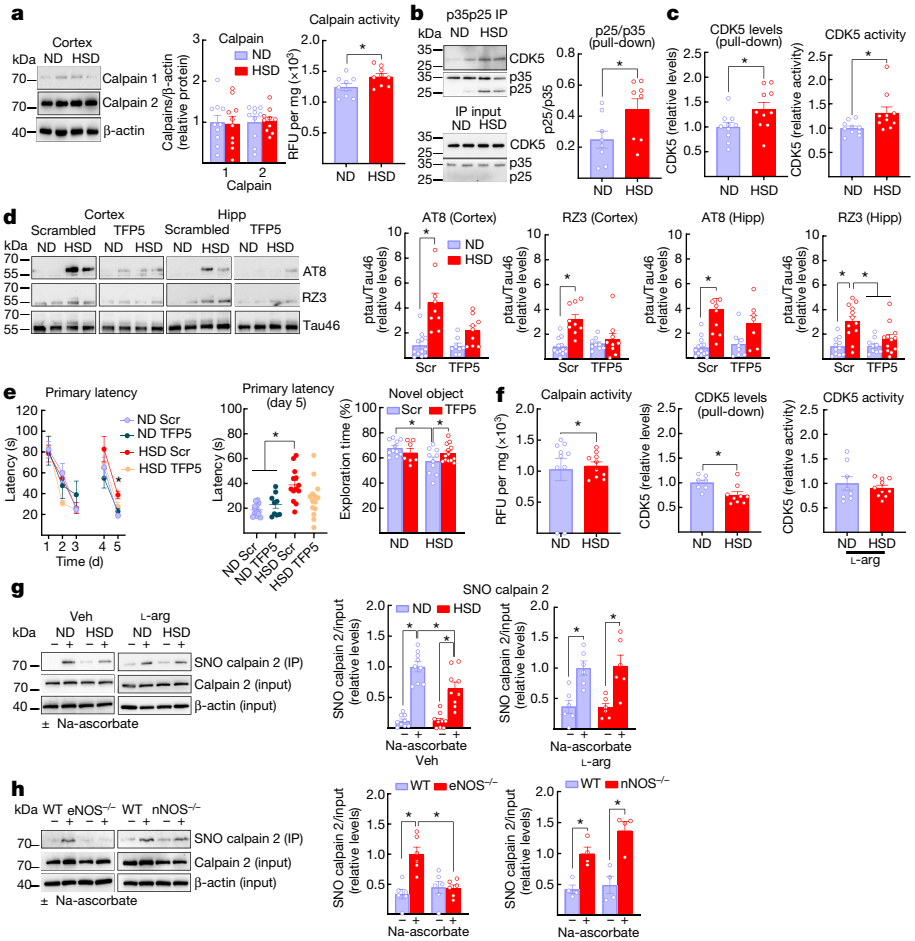

Fig. 3 | HSD induces activation of calpain and CDK5 associated with calpain denitrosylation. a, HSD did not alter expression of calpain 1 or 2 (ND/HSD, $n = 10$), but increased enzyme activity. ND/HSD $n = 9/9$, $^*P = 0.0404$ versus ND, two-tailed unpaired *t*-test. **b**, HSD increases the cleavage of p35 into p25. ND/HSD $n = 8/8$, $^*P = 0.0426$ versus ND, two-tailed unpaired *t*-test. **c**, HSD increases the level of CDK5 bound to p35p25 (ND/HSD $n = 10/10$, $^*P = 0.0347$) and CDK5 activity (ND/HSD $n = 10/10$, $^*P = 0.0274$; two-tailed unpaired *t*-test for HSD versus ND). **d**, The CDK5 peptide inhibitor TFP5 counteracts the HSD-induced increase in AT8 and RZ3 immunoreactivity. AT8, cortex: ND/HSD scrambled $n = 10/9$, ND/HSD TFP5 $n = 9/9$, diet: $^*P < 0.0001$, treatment: $^*P = 0.0164$; AT8, hippocampus: ND/HSD scrambled $n = 11/10$, ND/HSD TFP5 $n = 10/7$, diet: $^*P = 0.0004$, treatment: $^*P = 0.0360$; RZ3, cortex: ND/HSD scrambled $n = 10/10$, ND/HSD TFP5 $n = 10/11$, diet: $^*P < 0.0001$, treatment: $^*P = 0.0814$; RZ3, hippocampus: ND/HSD scrambled $n = 12/11$, ND/HSD TFP5 $n = 10/12$, diet: $^*P < 0.0001$, treatment: $^*P = 0.0066$; two-way ANOVA and Tukey's test. **e**, TFP5 rescues the spatial memory deficits induced by HSD. Primary latency, diet: $P = 0.6415$, time: $^*P < 0.0001$, two-way repeated measures ANOVA and Tukey's test; primary latency day 5, diet: $^*P = 0.0016$, treatment: $P = 0.5797$; two-way ANOVA and Tukey's test). TFP5 also improves cognitive performance of HSD-fed mice on the NOR test. Diet: $^*P = 0.0383$, treatment: $P = 0.1488$; two-way ANOVA and Tukey's test. **f**, L-Arginine counteracts the increase in calpain (ND/HSD $n = 8/10$, $^*P = 0.0335$ versus ND, two-tailed unpaired *t*-test) and CDK5 activity induced by HSD and reduces CDK5 bound to p35p25 (ND/HSD $n = 7/9$, $^*P = 0.0137$ versus ND, two-tailed unpaired *t*-test). **g**, Calpain 2 nitrosylation is reduced by HSD (ND/HSD $n = 9/9$, diet: $^*P = 0.0189$; ascorbate: $^*P < 0.0001$; two-way ANOVA and Tukey's test) and this effect is reversed by L-arginine. ND/HSD $n = 6/6$, diet: $P = 0.9487$, ascorbate: $^*P < 0.0001$, two-way ANOVA and Tukey's test. **h**, Nitrosylation is suppressed in eNOS$^{-/-}$ (ND/HSD $n = 6/6$, genotype: $^*P = 0.0223$, ascorbate: $^*P = 0.0021$, two-way ANOVA and Tukey's test), but not in nNOS$^{-/-}$ mice (ND/HSD $n = 4/4$, genotype: $P = 0.0843$, ascorbate: $P < 0.0001$; two-way ANOVA and Tukey's test). For gel source data see Supplementary Fig. 1. Data are expressed as mean ± s.e.m.

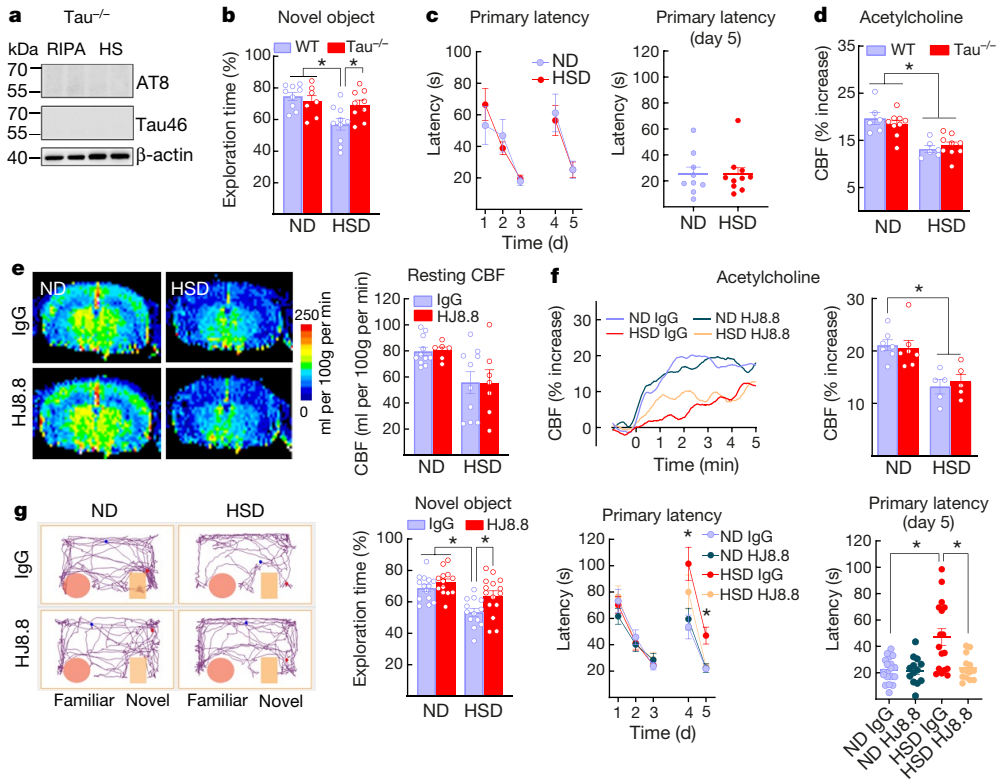

Fig. 4 | HSD-induced cognitive dysfunction is not observed in tau$^{-/-}$ mice and is prevented by tau antibodies despite cerebrovascular insufficiency. a, AT8 and Tau46 are absent in tau$^{-/-}$ mice in RIPA and heat-stable (HS) RIPA fractions. Representative blots from $n = 5$ ND-fed tau$^{-/-}$ mice. **b**, **c**, HSD does not alter cognition in tau$^{-/-}$ mice on the NOR test (wild-type (WT): ND/HSD $n = 9/10$; tau$^{-/-}$: ND/HSD $n = 7/9$; diet: $^*P = 0.0055$, genotype: $P = 0.1827$, two-way ANOVA and Tukey's test) or the Barnes maze (ND/HSD $n = 9/10$, diet: $P = 0.9348$, time: $^*P < 0.0001$, two-way ANOVA and Tukey's test). **d**, The increase in CBF produced by neocortical application of acetylcholine is reduced in tau$^{-/-}$ mice (ND/HSD wild-type, $n = 6/6$, tau$^{-/-}$, $n = 9/9$; diet: $^*P < 0.0001$, genotype: $P = 0.7920$, two-way ANOVA and Tukey's test). **e**, Anti-tau antibodies (HJ8.8, 50 mg per kg per week, intraperitoneal injection) do not prevent the reduction in resting CBF induced by HSD (IgG: ND/HSD $n = 11/9$; HJ8.8: ND/HSD $n = 6/5$; diet: $^*P = 0.0061$, treatment: $P = 0.9367$, two-way ANOVA and Tukey's test). **f**, HJ8.8 does not rescue the CBF response to acetylcholine (IgG: ND/HSD $n = 5/5$; HJ8.8: ND/HSD $n = 5/5$; diet: $^*P = 0.0005$, treatment: $P = 0.8516$, two-way ANOVA and Tukey's test). **g**, HJ8.8 ameliorates the cognitive dysfunction induced by HSD on both the NOR test (IgG: ND/HSD $n = 15/13$; HJ8.8: ND/HSD $n = 13/15$; diet: $^*P = 0.0001$, treatment: $^*P = 0.0054$, two-way ANOVA and Tukey's test) and the Barnes maze test (primary latency: IgG: ND/HSD $n = 19/15$; HJ8.8: ND/HSD $n = 13/14$; time: $^*P < 0.0001$, diet: $^*P = 0.0358$, two-way repeated measures ANOVA and Tukey's test; primary latency day 5: IgG: ND/HSD $n = 19/16$; HJ8.8: ND/HSD $n = 13/14$; $^*P = 0.0202$, Kruskal–Wallis and Dunn's test). Images on left show representative tracks. For gel source data see Supplementary Fig. 1. Data are expressed as mean ± s.e.m.

mice with arterial hypertension induced by angiotensin-II (Extended Data Fig. 3d, e) or in a model of Aβ accumulation (Tg2576 mice; Extended Data Fig. 3f), both of which are associated with endothelial dysfunction and cognitive impairment[19,20].

To determine whether an HSD alters the solubility of tau—a key determinant of its harmful effects[16]—we measured tau levels in brain tissue after sequential biochemical extraction in RAB (salt buffer), RIPA (detergent buffer) or 70% formic acid (FA), which contain, respectively, soluble, less soluble and highly insoluble tau. In samples taken from mice after 12 weeks of the HSD, tau in the RIPA and FA fractions was increased over that in samples from mice fed a normal diet, reflecting an increase in insoluble tau (Fig. 1g–i). Hypothermia, which does not cause cognitive impairment, also increased p-tau[21], but, unlike the HSD, did not lead to an increase in insoluble species (Extended Data Fig. 3g, h). These observations indicate that an HSD not only promotes hyperphosphorylation of tau, but also its aggregation.

As the nitric oxide precursor L-arginine counteracts the endothelial nitric oxide deficit in mice fed an HSD[7], mice were given L-arginine in their drinking water (10 g l^{-1}) during the last 4 weeks of the 12-week HSD course. L-Arginine suppressed accumulation of p-tau and prevented HSD-induced cognitive dysfunction (Fig. 2a–e, Extended Data Fig. 4a), without affecting the HSD-induced increase in circulating IL-17 (Extended Data Fig. 4b). Consistent with a key role of endothelial nitric oxide deficiency in accumulation of p-tau, eNOS-null (*Nos3*$^{-/-}$) mice fed a normal diet showed elevated p-tau that was not increased further by an HSD (Extended Data Fig. 4c, d).

Cyclin-dependent kinase 5 (CDK5), a kinase that is responsible for tau hyperphosphorylation[16], is tightly regulated by its binding partner p35[22,23]. Calpains cleave p35 bound to CDK5 into p25, which results in dysregulated activation of CDK5 and hyperphosphorylation of tau[22,23]. As reduced endothelial nitric oxide may lead to tau phosphorylation by activating CDK5 via p25[24], we investigated whether the HSD influenced the activity of calpain and CDK5. Calpain 2 is more abundant than calpain 1 in the neocortex (Fig. 3a) and is colocalized with CDK5 in neurons (Extended Data Fig. 4e, f). Mice fed an HSD showed increased calpain activity compared to mice fed a normal diet, and this led to an increase in the p25/p35 ratio and activation of CDK5 (Fig. 3a–c). Other CDK5 substrates besides tau, such as DARPP-32[25], were not phosphorylated (Extended Data Fig. 4g). Administration of the CDK5 peptide inhibitor TFP5 (40 mg kg^{-1} twice per week; intraperitoneal)[26] attenuated phosphorylation of tau and prevented cognitive dysfunction (Fig. 3d, e), without blunting the HSD-induced increase in circulating IL-17 (Extended Data Fig. 4h). L-Arginine prevented the HSD-induced activation of calpain and CDK5 (Fig. 3f) but did not alter calpain levels (Extended Data Fig. 4i).

The HSD did not increase the activity of GSK3β, an enzyme that has been implicated in tau phosphorylation[16], or the expression of the prolyl *cis/trans* isomerase PIN-1, which regulates tau dephosphorylation[27] (Extended Data Fig. 5a, b).

When calpain has been activated by Ca^{2+} it is regulated mainly by its endogenous inhibitor calpastatin and by nitrosylation by nitric oxide[28], which suppresses its activity[29]. As the HSD did not reduce calpastatin expression (Extended Data Fig. 5c), we used the biotin switch assay to investigate the effect of an HSD on calpain nitrosylation. Calpain nitrosylation was reduced in mice fed an HSD compared with mice fed a normal diet, and this effect was reversed by L-arginine (Fig. 3g). Nitrosylation was markedly suppressed in eNOS-null mice, but not in nNOS-null ($Nos1^{-/-}$) mice, attesting to the key role of eNOS-derived nitric oxide in regulating nitrosylation and activity of calpain (Fig. 3h). As the HSD reduced CDK5 nitrosylation (Extended Data Fig. 5d), it is unlikely that this modification, which activates the enzyme[30], is involved in the effects of the HSD.

Finally, we used tau-null ($Mapt^{-/-}$) mice and anti-tau antibodies to examine the relative contributions of p-tau and neurovascular dysfunction to the cognitive deficits induced by an HSD. Tau-null mice that were fed an HSD for 12 weeks did not exhibit cognitive impairment, but still showed a marked attenuation of the increase in CBF evoked by neocortical application of acetylcholine (Fig. 4a–d), a response mediated by eNOS-derived nitric oxide[31]. Similarly, wild-type mice treated with anti-tau antibodies (HJ8.8)[32] or control IgG (50 mg per kg per week; intraperitoneal) for the last 4 weeks of the 12-week HSD regimen showed improved cognitive function (Fig. 4g) compared with untreated mice, despite having reduced resting CBF and an attenuated CBF response to acetylcholine (Fig. 4e, f). HJ8.8 lowered p-tau in the hippocampus (measured by AT8 immunoreactivity; Extended Data Fig. 5e) but did not blunt the HSD-induced increase in circulating IL-17 (Extended Data Fig. 5f). The HSD did not affect the increase in CBF induced by neural activity in either tau-null mice or mice treated with HJ8.8 (Extended Data Fig. 5g)

These observations indicate that the cognitive dysfunction associated with HSD is mediated by a deficit in endothelial nitric oxide that results from denitrosylation of calpain. This deficit leads to activation of CDK5 and phosphorylation of tau in neurons (Extended Data Fig. 5h). Notably, the hypoperfusion and neurovascular dysfunction that also result from the endothelial nitric oxide deficit do not mediate the cognitive impairment. Rather, other aspects of endothelial function are involved—namely, endothelial nitric oxide maintaining calpain homeostasis and preventing CDK5 dysregulation and tau hyperphosphorylation.

Although the HSD used in mice, in which the salt content is 8–16-fold higher than in normal mouse chow[7,17], may exceed the highest reported levels of human salt consumption (12.5–20 g per day or 3–5 times the recommended level of 4–5 g per day)[33], our data provide a previously unrecognized link between dietary habits, vascular dysfunction and tau pathology, independent of cerebral hypoperfusion. Such relationships may play a role in the frequent coexistence of vascular and neurogenerative pathologies in conditions that cause dementia, such as Alzheimer's disease and frontotemporal dementia[12,13]. Whereas the avoidance of excessive salt consumption may help to prevent tau pathology, therapeutic efforts to counteract cerebrovascular dysfunction need to go beyond rescuing cerebral perfusion and target vascular mediators that govern the neurovascular interactions that are essential for cognitive health.

Online content

Any methods, additional references, Nature Research reporting summaries, source data, extended data, supplementary information, acknowledgements, peer review information; details of author contributions and competing interests; and statements of data and code availability are available at https://doi.org/10.1038/s41586-019-1688-z.

1. Scarmeas, N., Anastasiou, C. A. & Yannakoulia, M. Nutrition and prevention of cognitive impairment. *Lancet Neurol*. **17**, 1006–1015 (2018).
2. van de Rest, O., Berendsen, A. A., Haveman-Nies, A. & de Groot, L. C. Dietary patterns, cognitive decline, and dementia: a systematic review. *Adv. Nutr*. **6**, 154–168 (2015).
3. Kendig, M. D. & Morris, M. J. Reviewing the effects of dietary salt on cognition: mechanisms and future directions. *Asia Pac. J. Clin. Nutr*. **28**, 6–14 (2019).
4. De Strooper, B. & Karran, E. The cellular phase of Alzheimer's disease. *Cell* **164**, 603–615 (2016).
5. Nation, D. A. et al. Pulse pressure in relation to tau-mediated neurodegeneration, cerebral amyloidosis, and progression to dementia in very old adults. *JAMA Neurol*. **72**, 546–553 (2015).
6. Kim, H. J. et al. Assessment of extent and role of tau in subcortical vascular cognitive impairment using 18F-AV1451 positron emission tomography imaging. *JAMA Neurol*. **75**, 999–1007 (2018).
7. Faraco, G. et al. Dietary salt promotes neurovascular and cognitive dysfunction through a gut-initiated TH17 response. *Nat. Neurosci*. **21**, 240–249 (2018).
8. Fiocco, A. J. et al. Sodium intake and physical activity impact cognitive maintenance in older adults: the NuAge Study. *Neurobiol. Aging* **33**, 829.e821–829.e28, (2012).
9. Gardener, H., Rundek, T., Wright, C. B., Elkind, M. S. & Sacco, R. L. Dietary sodium and risk of stroke in the Northern Manhattan study. *Stroke* **43**, 1200–1205 (2012).
10. Blumenthal, J. A. et al. Lifestyle and neurocognition in older adults with cognitive impairments: a randomized trial. *Neurology* **92**, e212–e223 (2019).
11. Heye, A. K. et al. Blood pressure and sodium: association with MRI markers in cerebral small vessel disease. *J. Cereb. Blood Flow Metab*. **36**, 264–274 (2016).
12. Iadecola, C. The pathobiology of vascular dementia. *Neuron* **80**, 844–866 (2013).
13. Sweeney, M. D. et al. Vascular dysfunction—the disregarded partner of Alzheimer's disease. *Alzheimers Dement*. **15**, 158–167 (2019).
14. Shi, Y. et al. Cerebral blood flow in small vessel disease: a systematic review and meta-analysis. *J. Cereb. Blood Flow Metab*. **36**, 1653–1667 (2016).
15. Marshall, R. S. et al. Recovery of brain function during induced cerebral hypoperfusion. *Brain* **124**, 1208–1217 (2001).
16. Wang, Y. & Mandelkow, E. Tau in physiology and pathology. *Nat. Rev. Neurosci*. **17**, 5–21 (2016).
17. Zhao, Y. et al. Sodium intake regulates glucose homeostasis through the PPARδ/adiponectin-mediated SGLT2 pathway. *Cell Metab*. **23**, 699–711 (2016).
18. Min, S. W. et al. Critical role of acetylation in tau-mediated neurodegeneration and cognitive deficits. *Nat. Med*. **21**, 1154–1162 (2015).
19. Iadecola, C. et al. SOD1 rescues cerebral endothelial dysfunction in mice overexpressing amyloid precursor protein. *Nat. Neurosci*. **2**, 157–161 (1999).
20. Faraco, G. et al. Perivascular macrophages mediate the neurovascular and cognitive dysfunction associated with hypertension. *J. Clin. Invest*. **126**, 4674–4689 (2016).
21. Arendt, T., Stieler, J. T. & Holzer, M. Tau and tauopathies. *Brain Res. Bull*. **126**, 238–292 (2016).
22. Lee, M. S. et al. Neurotoxicity induces cleavage of p35 to p25 by calpain. *Nature* **405**, 360–364 (2000).
23. Patrick, G. N. et al. Conversion of p35 to p25 deregulates Cdk5 activity and promotes neurodegeneration. *Nature* **402**, 615–622 (1999).
24. Austin, S. A. & Katusic, Z. S. Loss of endothelial nitric oxide synthase promotes p25 generation and tau phosphorylation in a murine model of Alzheimer's disease. *Circ. Res*. **119**, 1128–1134 (2016).
25. Bibb, J. A. et al. Phosphorylation of DARPP-32 by Cdk5 modulates dopamine signalling in neurons. *Nature* **402**, 669–671 (1999).
26. Shukla, V. et al. A truncated peptide from p35, a Cdk5 activator, prevents Alzheimer's disease phenotypes in model mice. *FASEB J*. **27**, 174–186 (2013).
27. Kimura, T. et al. Isomerase Pin1 stimulates dephosphorylation of tau protein at cyclin-dependent kinase (Cdk5)-dependent Alzheimer phosphorylation sites. *J. Biol. Chem*. **288**, 7968–7977 (2013).
28. Ono, Y., Saido, T. C. & Sorimachi, H. Calpain research for drug discovery: challenges and potential. *Nat. Rev. Drug Discov*. **15**, 854–876 (2016).
29. Etwebi, Z., Landesberg, G., Preston, K., Eguchi, S. & Scalia, R. Mechanistic role of the calcium-dependent protease calpain in the endothelial dysfunction induced by MPO (myeloperoxidase). *Hypertension* **71**, 761–770 (2018).
30. Qu, J. et al. S-Nitrosylation activates Cdk5 and contributes to synaptic spine loss induced by β-amyloid peptide. *Proc. Natl Acad. Sci. USA* **108**, 14330–14335 (2011).
31. Iadecola, C. The neurovascular unit coming of age: a journey through neurovascular coupling in health and disease. *Neuron* **96**, 17–42 (2017).
32. Yanamandra, K. et al. Anti-tau antibodies that block tau aggregate seeding *in vitro* markedly decrease pathology and improve cognition *in vivo*. *Neuron* **80**, 402–414 (2013).
33. Powles, J. et al. Global, regional and national sodium intakes in 1990 and 2010: a systematic analysis of 24 h urinary sodium excretion and dietary surveys worldwide. *BMJ Open* **3**, e003733 (2013).

Methods

Most of the methods used in this study are well established in the laboratory and have been described in detail in previous publications[7,20,34]. Here we provide only a brief description.

Mice

All procedures were approved by the institutional animal care and use committee of Weill Cornell Medicine (animal protocol number: 0807-777A). Studies were conducted, according to the ARRIVE guidelines (https://www.nc3rs.org.uk/arrive-guidelines), in the following lines of mice: C57BL/6 (JAX), B6.129X1-Mapttm1Hnd ($Tau^{-/-}$, JAX, Stock #007251), B6.129P2-*Nos3*^{tm1Unc}/J ($eNOS^{-/-}$, JAX, Stock #002684), B6.129S4-*Nos1*^{tm1Plh}/J ($nNOS^{-/-}$, JAX, Stock #002986), 129S6.Cg-Tg(APPSWE) 2576Kha N20+? (Taconic, Stock #279) and Tg(Camk2a-tTA)*1Mmay Fgf14*$^{Tg(tetO\text{-}MAPT*P301L)4510Kha}$/J (rTg4510, JAX, Stock#024854). Unless otherwise indicated, 8-week-old male mice were used.

High-salt diet

Male or female mice (8 weeks old) received normal chow (0.5% NaCl) and tap water ad libitum (normal diet (ND)) or sodium-rich chow (4 or 8% NaCl) and tap water containing 1% NaCl ad libitum (HSD) for 4–36 weeks as stated[7].

In vivo treatments

The nitric oxide precursor L-arginine (10 g/l; Sigma) was administered in the drinking water starting after 8 weeks of HSD and continuing until 12 weeks. ND- and HSD-fed mice were treated (intraperitoneally (i.p.), weekly) with 50 mg/kg of anti-tau (HJ8.8) or mouse IgG1 isotype control (Clone MOPC-21; bioXcell) antibodies for the last 4 weeks of the HSD treatment period (12 weeks) before behavioural and cerebrovascular studies. HJ8.8 is a high-affinity antibody generated against human tau that can recognize both human and mouse tau (K_d (dissociation constant) = 0.926 nM to mouse tau). In other experiments, ND- and HSD-fed mice were treated (i.p. twice a week) with 40 mg/kg of TPF5 (KEAFWDRCLSVINLMSSKML-QINAYARAARRAARR) or scrambled peptide (GGGFWDRCLSGKGKMSSK-GGGINAYARAARRAARR) (Peptide 2.0)[35] for the last 4 weeks of the HSD treatment period (12 weeks) before behavioural and molecular studies.

General surgical procedures for CBF studies

Mice were anaesthetized with isoflurane (induction, 5%; maintenance, 2%). The trachea was intubated and mice were artificially ventilated with a mixture of N_2 and O_2. One of the femoral arteries was cannulated for recording mean arterial pressure (MAP) and collecting blood samples for blood gas analysis[36]. Rectal temperature was maintained at 37 °C. End tidal CO_2, monitored by a CO_2 analyser (Capstar-100, CWE Inc.), was maintained at 2.6–2.7% to provide a pCO_2 of 30–40 mm Hg and a pH of 7.3–7.437. After surgery, isoflurane was discontinued and anaesthesia was maintained with urethane (750 mg/kg, i.p.) and chloralose (50 mg/kg, i.p.). Throughout the experiment the level of anaesthesia was monitored by testing motor responses to a tail pinch.

Monitoring CBF

A small craniotomy (2 × 2 mm) was performed to expose the parietal cortex, the dura was removed and the site was superfused with Ringer's solution (37 °C; pH 7.3–7.4)[20]. CBF was continuously monitored at the site of superfusion with a laser-Doppler probe (Perimed) positioned stereotaxically ~0.5 mm above the cortical surface and connected to a data acquisition system (PowerLab). CBF values are expressed as percentage increases relative to the resting level.

Protocol for CBF experiments

After MAP and blood gases stabilized, CBF responses were recorded[7]. The whisker-barrel cortex was activated for 60 s by stroking the contralateral vibrissae, and the evoked changes in CBF were recorded. The endothelium-dependent vasodilator acetylcholine (ACh; 100 µM, Sigma) was superfused onto the exposed neocortex for 5 min and the associated changes in CBF were recorded by laser-Doppler flowmetry. CBF and MAP data were collected using Chart 5 Pro (v.5.5.6).

Measurement of resting CBF by ASL-MRI

CBF was assessed quantitatively using arterial spin labelling magnetic resonance imaging (ASL-MRI), performed on a 7.0-Tesla 70/30 Bruker Biospec small-animal MRI system with 450 mT/m gradient amplitude and a 4,500 T/m/s slew rate. A volume coil was used for transmission and a surface coil for reception. Anatomical localizer images were acquired to find the transversal slice approximately corresponding to bregma + 0.5 mm. This position was used for subsequent ASL-MRI, which was based on a flow-sensitive alternating inversion recovery rapid acquisition with relaxation enhancement (FAIR-RARE) pulse sequence labelling the inflowing blood by global inversion of the equilibrium magnetization. One axial slice was acquired with a field of view of 15 × 15 mm, spatial resolution of 0.117 × 0.117 × 1 mm, TE (echo time) of 5.368 ms, effective TE of 48.32 ms, recovery time of 10 s and a RARE (rapid imaging with refocused echoes) factor of 72. Twenty-two turbo inversion recovery values ranging from 30 to 2,300 ms were used, and the inversion slab thickness was 4 mm. For computation of resting CBF (rCBF), the Bruker ASL perfusion processing macro was used. It uses a published model[37] and includes steps to mask out the background. The masked rCBF images were exported to Analyze format on the MRI console. The ASL images were analysed by ImageJ and the average CBF value is reported as ml per 100 g of tissue per minute[7].

Osmotic minipump implantation for delivery of angiotensin-II

Osmotic minipumps containing vehicle (saline) or angiotensin-II (600 ng/kg/min) were implanted subcutaneously under isoflurane anaesthesia. Systolic blood pressure was monitored in awake mice using tail-cuff plethysmography[20]. Forty-two days later, mice were anaesthetized and their brains were collected for assessment of tau phosphorylation.

Hypothermia

C57BL/6 mice (12 weeks old) were anaesthetized by injection of ketamine/xylazine (100/10 mg/kg). Rectal temperature was continuously monitored and kept at 37 °C (normothermia) or 30 °C (hypothermia) using a thermostatically controlled heating pad. Mice were killed 30 min after anaesthesia and their brains were collected and frozen on dry ice. Tissues were kept at −80 °C until processing for immunoblot analysis.

Immunoblot analysis

Cortex (~80–90 mg) and hippocampus (~15 mg) isolated from ND- and HSD-fed mice were sonicated in 800 and 500 µl of RIPA buffer, respectively (50 mM Tris-HCl pH 8.0, 150 mM NaCl, 0.5% deoxycholic acid, 0.1% SDS, 1 mM EDTA pH 8.0, 1% IGEPAL CA-630, 1 mM Na_3VO_4, 20 mM NaF and one tablet per 10 ml of cOmplete, EDTA-free Protease Inhibitor Cocktail, Millipore Sigma) and equal volumes were mixed with SDS sample buffer, boiled and analysed on 10% or 10–20% Novex WedgeWell gels (Thermo Fisher Scientific). Proteins were transferred to PVDF membranes (Millipore), blocked at room temperature for 1 h with 5% milk in TBS, and incubated overnight at 4 °C, with primary antibodies (see Reporting Summary) in 5% BSA in TBS/0.1% Tween-20 (TBST). Membranes were washed in TBST and incubated with goat anti-mouse or rabbit secondary antibodies conjugated to horseradish peroxidase (Santa Cruz Biotechnology) for 1 h at room temperature, and protein bands were visualized with Clarity Western ECL Substrate (Bio Rad) on a Bio Rad ChemiDoc MP Imaging System. Quantification was performed using Image Laboratory v.6.0 (Bio Rad).

Preparation of heat-stable RIPA fractions for tau enrichment

After homogenization in cold RIPA buffer and centrifugation, 150 µl of the supernatant containing the proteins was boiled at 100 °C for 10 min.

Samples were cooled on ice for 20 min and then centrifuged at 20,000*g* at 4 °C for 15 min. The supernatant corresponding to the heat-stable fraction was then harvested. This method is used to isolate proteins resistant to heat, including tau and other microtubule-associated proteins. Thus, endogenous immunoglobulins are precipitated during the boiling process and eliminated from the supernatant. The proteins were then mixed with equal volumes of SDS sample buffer, boiled and analysed on 10% Novex WedgeWell gels (Thermo Fisher Scientific). Although tau protein is partially lost during the boiling process, the heat-stable samples are enriched with tau (Extended Data Fig. 5h). Furthermore, boiling substantially improves the specificity of certain antibodies, such as AT8, RZ3 or MC1[38].

Tau dephosphorylation

After overnight dialysis to remove phosphatase inhibitors, protein samples (40 µl) were incubated with 5 µl of 10× NEBuffer for Protein MetalloPhosphatases (PMP), 5 µl of 10 mM $MnCl_2$ and 1 µl of Lambda protein phosphatase (Lambda PP, New England Biolabs) at 30 °C for 3 h. Reactions were stopped by addition of SDS sample buffer and boiling for 5 min at 100 °C.

Brain tissue protein extraction

Extraction was performed as described previously[32]. The cortex (~80–90 mg) and hippocampus (~15 mg) of each brain were homogenized by sonication in 800 and 300 µl, respectively, of RAB buffer (100 mM MES, 1 mM EDTA, 0.5 mM $MgSO_4$, 750 mM NaCl, 20 mM NaF, 1 mM Na_3VO_4, supplemented by EDTA-free Protease Inhibitor Cocktail, Millipore Sigma). In brief, the samples were centrifuged at 50,000*g* for 20 min at 4 °C using an Optima MAX-TLA 120.2 Ultracentrifuge (Beckman). The supernatants were collected as RAB-soluble fractions and pellets were resuspended in identical volumes of RIPA buffer (150 mM NaCl, 50 mM Tris, 0.5% deoxycholic acid, 1% Triton X-100, 0.5% SDS, 25 mM EDTA, pH 8.0, 20 mM NaF, 1 mM Na_3VO_4 supplemented by EDTA-free Protease Inhibitor Cocktail, Millipore Sigma), and centrifuged at 50,000*g* for 20 min at 4 °C. The supernatants were collected as RIPA-soluble fractions. The pellets were sonicated in 70% FA (300 µl for cortex and 125 µl for hippocampus), and centrifuged at 50,000*g* for 20 min at 4 °C. The supernatants were collected as 70% FA fractions. All fractions were stored at −80 °C until analysed. For western blotting, an aliquot of 100 µl of the FA fractions was evaporated in a Savant SpeedVac concentrator at 45 °C for 1 h. The samples were resuspended in 100 µl SDS sample buffer with the addition of 1 µl of 10 N NaOH, sonicated and then boiled for 5 min.

Measurement of tau, Aβ and IL-17

Tau, Aβ and IL-17 were measured using an electrochemiluminescence-based multi-array method through the Quickplex SQ 120 system (Meso Scale Diagnostics LLC). Tau and Aβ peptide levels (Aβ38, Aβ40 and Aβ42) were measured in the RAB, RIPA and FA fractions of both cortex and hippocampus using the MSD Mouse Total Tau (K151DSD) and MSD V-PLEX Aβ Peptide Panel 1 (4G8) (K15199) kits according to the manufacturer's protocol. IL-17A was measured in the serum of ND- and HSD-fed mice using the MSD V-PLEX Mouse IL-17A Kit (K152RFD) according to the manufacturer's protocol.

Immunohistochemistry

After 12 weeks of ND or HSD, mice were anaesthetized with intraperitoneal pentobarbital (200 mg/kg), and then perfused transcardiacally with cold PBS, followed by cold 4% paraformaldehyde (PFA) in PBS. The brains were removed and immersed first in 4% PFA overnight and then in 70% ethanol for 3 days. Brains were then embedded in paraffin and cut into 6-µm sections using a microtome. After rehydration and antigen retrieval in preheated citrate buffer (10 µM) for 30 min, brain sections were immersed in 3% H_2O_2 and then blocked with 100% Sniper (Biocare Medical) for 1 h. After blocking, sections were incubated for 2.5 days at 4 °C with the AT8 and MC1 antibodies (1:250 and 1:100 in 1:50 Sniper in PBS, respectively) and thereafter processed for 1 h with the biotinylated secondary antibody in 1% normal donkey serum PBS (anti-mouse IgG1, Jackson ImmunoResearch). Reactions were visualized with the ABC-complex (Vectorlabs) and 3,3-diaminobenzidine. A Nikon light microscope was used to visualize the signal associated with each antibody.

Immunofluorescence

After 12 weeks of ND or HSD, mice were anaesthetized with intraperitoneal pentobarbital (200 mg/kg), and then perfused transcardiacally with cold PBS, followed by cold 4% paraformaldehyde (PFA) in PBS. The brains were removed and immersed first in 4% PFA overnight. Sections (thickness, 40 µm) were cut through the whole brain using a vibratome. After blocking with 5% normal donkey serum in 0.5% Triton-X/PBS, sections were incubated over the weekend at 4 °C with antibodies against NEUN (1:200, mouse, Millipore Sigma, MAB377), GFAP (1:200, mouse, Millipore Sigma, G3893), IBA1 (1:200, rabbit, Wako, 019-19741), CD13 (1:200, goat, R&D Systems, AF2335), calpain 2 (1:100, rabbit, Santa Cruz, sc-373966) or CDK5 (1:100, rabbit, Santa Cruz, sc-6247) in 0.5% Triton-X in PBS and thereafter processed for 2 h with FITC, Cy3 or Cy5 secondary antibodies in 0.5% Triton-X in PBS. An epifluorescence microscope (IX83 Inverted Microscope, Olympus) or a confocal microscope (Leica TCS SP5) was used to visualize the signal associated with each antibody.

Fluoro-Jade B staining

After rehydration, brain sections (6 µm) were immersed in 1% sodium hydroxide in 80% alcohol for 5 min, followed by 2 min in 70% alcohol and 2 min in distilled water. The slides were transferred to a solution of 0.06% potassium permanganate for 10 min on a shaker. After rinsing for 2 min in distilled water, the slides were immersed in the staining solution (0.0004% Fluoro-Jade B, Millipore Sigma, in 0.1% acetic acid) for 20 min in the dark. Finally, the slides were rinsed three times for 1 min in distilled water and then placed on a slide warmer, set at approximately 50 °C, until they were fully dry. The dry slides were cleared by immersion in xylene for at least a minute before coverslipping with DPX (Sigma).

TUNEL staining

After rehydration and antigen retrieval according to the manufacturer's protocol (In situ Cell Death Detection Kit, Fluorescein, Roche, #11 684 795 910), brain sections were blocked for 30 min in Tris-HCl, 0.1 M pH 7.5, containing 3% BSA and 20% normal donkey serum and then incubated with the TUNEL reaction mixture for 60 min at 37 °C in a humidified atmosphere in the dark. After washing, slides were evaluated by an epifluorescence microscope (IX83 Inverted Microscope, Olympus). A positive control was obtained by pre-incubating brain slices with DNase I recombinant (3,000 U/ml in 50 mM Tris-HCl, pH 7.5, 1 mg/ml BSA), for 10 min at room temperature, to induce DNA strand breaks.

Klüver–Barrera white-matter staining

The Klüver–Barrera stain was performed using the Luxol Fast Blue Stain Kit (ScyTek Laboratory Inc.). Brains were removed after transcardiac perfusion with PBS and 4% PFA and sectioned with a vibratome (thickness, 40 µm), and the positive (blue-stained) area in the corpus callosum was quantified by ImageJ.

Thioflavin S staining

After mounting on slides and post-fixation with 4% PFA in PBS for 10 min, coronal brain sections (40 µm) were washed and labelled with 0.05% (w/v) thioflavine-S in 50% (v/v) ethanol for 10 min as previously described[39]. An epifluorescence microscope (IX83 Inverted Microscope, Olympus) was used to visualize the FITC signal associated with thioflavine-S.

Calpain activity

Calpain activity was measured using a Calpain Activity Assay Kit from AbCam[40,41]. In brief, fresh cortex and hippocampus were homogenized

in the extraction buffer provided with the kit, which specifically extracts cytosolic proteins without contamination of cell membrane or lysosome proteases and prevents auto-activation of calpain during the extraction procedure. The fluorometric assay is based on the detection of cleavage of the calpain substrate Ac-LLY-AFC. Ac-LLY-AFC emits blue light (λ_{max} = 400 nm); upon cleavage of the substrate by calpain, free AFC emits a yellow-green fluorescence (λ_{max} = 505 nm), which can be quantified using a fluorometer or a fluorescence plate reader. The specificity of the signal was confirmed using the calpain inhibitor Z-LLY-FMK (100–200 μM). The activity is expressed as relative fluorescent units (RFU) per milligram of protein for each sample.

p35/p25 and GSK3β immunoprecipitation

Immunoprecipitation was performed with anti-p35p25 (Cell Signaling), anti-GSK3β (Cell Signaling) or anti-rabbit monoclonal IgG1 isotype control antibodies (Santa Cruz Biotechnology). Samples were incubated overnight with the primary antibodies and then with protein-A sepharose (p35p25) (GE Healthcare Life Sciences) or protein-G Dynabeads (GSK3β) (Thermo Fisher Scientific) for 2 h at 4 °C. Precipitates were used for measurement of CDK5 or GSK3β activity. Immunoprecipitation was confirmed by loading the samples onto 10% Tris-glycine SDS polyacrylamide gels and western blotting as described above.

Detection of *S*-nitrosylation with the biotin-switch technique

S-nitrosylated calpain 2 was detected using the biotin-switch technique, as previously described[42]. In brief, samples were sonicated in 800 μl of RIPA buffer containing 0.1 mM neocuproine and, after centrifugation, protein concentrations were measured. Cysteine thiol groups in 1 mg of proteins were blocked with 10% *S*-methylmethane thiosulfonate (MMTS) (Sigma). After protein-precipitation with 100% acetone, sodium ascorbate was added to the sample to convert each *S*-nitrothiol (SNO) to a free thiol via a transnitrosation reaction to generate *O*-nitrosoascorbate. Next, each nascent free thiol (previously an SNO site) was biotinylated with biotin–HPDP (Pierce). Biotinylated proteins were then pulled down using avidin beads and analysed on 10% Novex WedgeWell gels (Thermo Fisher Scientific). Before avidin pull-down, a small fraction of each sample was collected to determine protein 'input'. The degree of pull-down correlates with protein *S*-nitrosylation of calpain 2 or CDK5, which was detected with an antibody against the two proteins. Nitrosylation of calpain 2 or CDK5 is expressed as the ratio between the pull-down signal and the input corrected for β-actin levels.

CDK5 and GSK3β activity

CDK5 activity in brain lysates was determined after pull-down with p25/p35 antibody (Cell Signaling) from 500 μg total protein using a synthetic histone H1 peptide substrate (PKTPKKAKKL, Enzo Life Sciences). GSK3β activity was determined after pull-down with GSK3β antibody (Cell Signaling) from 100 μg total protein using phospho-glycogen synthase peptide-2a as substrate (Tocris). Phosphorylation reactions were initiated by mixing bead-coupled CDK5 with 40 μl reaction buffer containing the following: 50 mM HEPES.KOH (pH 7.4), 5 mM $MgCl_2$, 0.05% BSA, 50 μM substrate, 50 μM cold ATP, 1 mM dithiothreitol, 1× complete protease inhibitors without EDTA (Roche Applied Biosciences) and 5 Ci/mmole $^{\gamma 32}$P-ATP. Companion reactions for every sample were executed in the presence of the CDK5 inhibitor ((R)-CR8, Tocris) (10 μM) or the GSK3β inhibitor (CHIR 99021, Tocris) (10 μM) to correct for non-specific activity. Reactions were incubated at 30 °C for 30 min, after which they were terminated by spotting on P81 phosphocellulose cation-exchange chromatography paper. Filters were washed four times for 2 min in 0.5% phosphoric acid, and the remaining radioactivity was quantified in a scintillation counter by the Cherenkov method.

Novel object recognition test

The NOR test was conducted under dim light in a plastic box. Stimuli consisted of plastic objects that varied in colour and shape but had similar sizes[43,44]. A video camera mounted on the wall directly above the box was used to record the testing session for off-line analysis. Mice were acclimated to the testing room and chamber for one day before testing. Twenty-four hours after habituation, mice were placed in the same box in the presence of two identical sample objects and were allowed to explore for 5 min. After an intersession interval of 24 h, mice were placed in the same box but one of the two objects was replaced by a novel object. Mice were allowed to explore for 5 min. Exploratory behaviour was later assessed manually by an experimenter blinded to the treatment group. Exploration of an object was defined as the mouse sniffing the object or touching the object while looking at it. Placing the forepaws on the objects was considered as exploratory behaviour but climbing on the objects was not. A minimal exploration time for both objects (total exploration time) during the test phase (~5 s) was used. The amount of time taken to explore the novel object was expressed as a percentage of the total exploration time and provides an index of recognition memory[43,44]. Any-Maze v5.3 was used for collection and analysis of the behavioural data.

The Barnes maze test

The Barnes maze consisted of a circular open surface (90 cm in diameter) elevated to 90 cm on four wooden legs[45]. There were 20 circular holes (5 cm in diameter) equally spaced around the perimeter, and positioned 2.5 cm from the edge of the maze. No wall and no intra-maze visual cues were placed around the edge. A wooden plastic escape box (11 × 6 × 5 cm) was positioned beneath one of the holes. Two neon lamps and a buzzer were used as aversive stimuli. The Any-Maze tracking system (Stoelting) was used to record the movement of mice on the maze. Extra-maze visual cues consisted of objects within the room (table, computer, sink, door and so on) and the experimenter. Mice were tested in groups of seven to ten, and between trials they were placed into cages, which were placed in a dark room adjacent to the test room for the inter-trial interval (20–30 min). No habituation trial was performed. The acquisition phase consisted of three consecutive training days with three trials per day with the escape hole located at the same location across trials and days. On each trial a mouse was placed into a start tube located in the centre of the maze, the start tube was raised, and the buzzer was turned on until the mouse entered the escape hole. After each trial, mice remained in the escape box for 60 s before being returned to their cage. Between trials the maze floor was cleaned with 10% ethanol in water to minimize olfactory cues. For each trial mice were given 3 min to locate the escape hole, after which they were guided to the escape hole or placed directly into the escape box if they failed to enter the escape hole. Four parameters of learning performance were recorded: (1) the latency to locate (primary latency) and (2) enter the escape hole (total latency), (3) the number of errors made and (4) the distance travelled before locating the escape hole[45]. When a mouse dipped its head into a hole that did not provide escape, it was considered an error. On days 4 and 5, the location of the escape hole was moved 180° from its previous location (reverse learning) and two trials per day were performed. Any-Maze v.5.3 was used for collection and analysis of the behavioural data.

Statistics

Sample size was determined using power analysis based on work previously published by our laboratory on the effects of dietary salt on CBF regulation and cognitive function[7]. On these bases, 10–15 mice per group were required in studies involving assessment of cognitive function and cerebrovascular function[7,20]. Mice were randomized to the different experimental conditions and treatments using the random number generator function (RANDBETWEEN) in Microsoft Excel. Analysis of the data was performed in a blinded fashion using GraphPad Prism (v.7.0). All data were tested for normal distribution using the Shapiro–Wilk test. Intergroup differences were analysed using the two-tailed unpaired *t*-test for single comparison or using one- or two-way ANOVA (with Tukey's or

Bonferroni's post-hoc analysis) for multiple comparisons. Non-normally distributed data were tested using the Mann–Whitney *U* test for single comparison or the Kruskal–Wallis test for multiple comparisons. Data are expressed as mean ± s.e.m. and differences are considered statistically significant at $P < 0.05$.

Reporting summary

Further information on research design is available in the Nature Research Reporting Summary linked to this paper.

Data availability

Source data include final quantifications from in vivo animal work.

34. Hochrainer, K. et al. The ubiquitin ligase HERC3 attenuates NF-κB-dependent transcription independently of its enzymatic activity by delivering the RelA subunit for degradation. *Nucleic Acids Res*. **43**, 9889–9904 (2015).
35. Shukla, V. et al. TFP5, a peptide inhibitor of aberrant and hyperactive Cdk5/p25, attenuates pathological phenotypes and restores synaptic function in CK-p25Tg mice. *J. Alzheimers Dis*. **56**, 335–349 (2017).
36. Faraco, G. et al. Circulating endothelin-1 alters critical mechanisms regulating cerebral microcirculation. *Hypertension* **62**, 759–766 (2013).
37. Kober, F. et al. High-resolution myocardial perfusion mapping in small animals in vivo by spin-labeling gradient-echo imaging. *Magn. Reson. Med*. **51**, 62–67 (2004).
38. Petry, F. R. et al. Specificity of anti-tau antibodies when analyzing mice models of Alzheimer's disease: problems and solutions. *PLoS One* **9**, e94251 (2014).
39. Faraco, G. et al. Hypertension enhances Aβ-induced neurovascular dysfunction, promotes β-secretase activity, and leads to amyloidogenic processing of APP. *J. Cereb. Blood Flow Metab*. **36**, 241–252 (2016).
40. Voit, A. et al. Reducing sarcolipin expression mitigates Duchenne muscular dystrophy and associated cardiomyopathy in mice. *Nat. Commun*. **8**, 1068 (2017).
41. Liu, W. et al. Metabolic stress-induced cardiomyopathy is caused by mitochondrial dysfunction due to attenuated Erk5 signaling. *Nat. Commun*. **8**, 494 (2017).
42. Forrester, M. T., Foster, M. W., Benhar, M. & Stamler, J. S. Detection of protein S-nitrosylation with the biotin-switch technique. *Free Radic. Biol. Med*. **46**, 119–126 (2009).
43. Cohen, S. J. & Stackman, R. W. Jr Assessing rodent hippocampal involvement in the novel object recognition task. A review. *Behav. Brain Res*. **285**, 105–117 (2015).
44. Grayson, B. et al. Assessment of disease-related cognitive impairments using the novel object recognition (NOR) task in rodents. *Behav. Brain Res*. **285**, 176–193 (2015).
45. O'Leary, T. P. & Brown, R. E. Optimization of apparatus design and behavioral measures for the assessment of visuo-spatial learning and memory of mice on the Barnes maze. *Learn. Mem*. **20**, 85–96 (2013).

Acknowledgements We thank P. Davies for providing the RZ3, MC1 and PHF1 antibodies and Y. Li for sharing the Quickplex SQ 120 system (Meso Scale Diagnostics LLC). This study was supported by National Institutes of Health grants R37-NS089323 (C.I.) and 1R01-NS095441 (C.I.), by a grant from the Cure Alzheimer's Fund (G.F. and C.I.) and by a Scientist Development Grant from the American Heart Association (G.F.). Support from the Feil Family Foundation is gratefully acknowledged.

Author contributions G.F. performed western blotting experiments, behavioural tests and cerebrovascular studies, and analysed data. K.H. performed experiments on CDK5 and GSK3β activity and analysed data. S.G.S. performed western blotting experiments, behavioural tests and immunohistochemistry. S.S. and M.M.S. performed experiments on the effects of hypertension on tau. A.M. performed immunohistochemistry experiments. H.J. and D.M.H. provided the HJ8.8 antibody. J.A. supervised the molecular aspects of the study and edited the manuscript. G.F. and C.I. designed and supervised the entire study and wrote the manuscript.

Competing interests D.M.H. is listed as an inventor on a patent licensed by Washington University to C2N Diagnostics and subsequently AbbVie on the therapeutic use of anti-tau antibodies; co-founded and is on the scientific advisory board of C2N Diagnostics; and is on the scientific advisory board of Denali, Genentech, and Proclara. C.I. is on the scientific advisory board of Broadview Ventures.

Additional information

Supplementary information is available for this paper at https://doi.org/10.1038/s41586-019-1688-z.

Correspondence and requests for materials should be addressed to G.F. or C.I.

Peer review information *Nature* thanks Nikolaos Scarmeas, Berislav Zlokovic and the other, anonymous, reviewer(s) for their contribution to the peer review of this work.

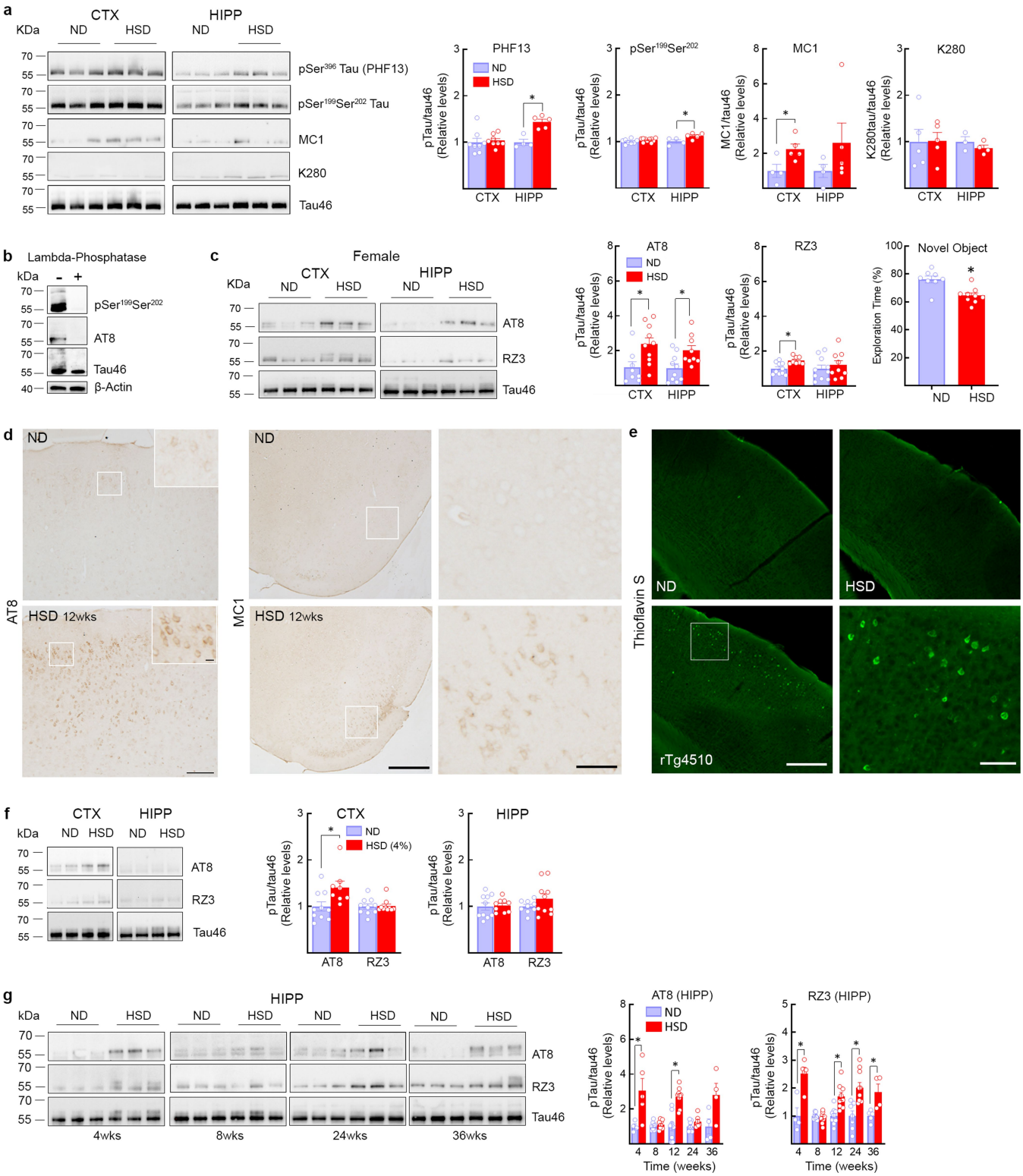

Extended Data Fig. 1 | See next page for caption.

Extended Data Fig. 1 | HSD (4 or 8%) induced tau phosphorylation: brain localization, sex differences and time course. a, HSD (8% NaCl) increases tau phosphorylation on Ser396 (PHF13) and on Ser199Ser202 in the hippocampus (HIPP) but not in the neocortex (CTX) (HIPP: PHF13, ND/HSD $n = 4/5$, $^*P = 0.0016$; $Ser^{199}Ser^{202}$, ND/HSD $n = 4/5$, $^*P = 0.0337$; two-tailed unpaired *t*-test versus ND), whereas acetylation of tau on Lys280 (K280) is not affected. MC1 immunoreactivity increases in both neocortex and hippocampus in HSD-fed mice but reaches statistical significance only in neocortex (MC1, ND/HSD $n = 4/5$, $^*P = 0.0321$ versus ND, two-tailed unpaired *t*-test). **b**, Tau phosphorylation on Ser199Ser202 and Ser202Thr205 is abolished after treatment of brain samples with lambda phosphatase. **c**, HSD increases AT8 immunoreactivity (left graph) in neocortex and hippocampus of female mice, but RZ3 (middle) increases only in neocortex (AT8, cortex: ND/HSD $n = 8/10$, $^*P = 0.0159$; hippocampus: ND/HSD $n = 10/9$, $^*P = 0.0151$; RZ3, cortex: ND/HSD $n = 10/8$, $^*P = 0.0117$; two-tailed unpaired *t*-test for HSD versus ND). Right, HSD induces a deficit in NOR in female mice (ND/HSD $n = 8/9$, $^*P = 0.0017$ versus ND, two-tailed unpaired *t*-test). **d**, HSD increases AT8 immunoreactivity in neuronal cell bodies of the somatosensory cortex (scale bars, 100 µm (main images); 10 µm (insets)) and MC1 immunoreactivity in neuronal bodies of the pyriform cortex (scale bars, 500 µm (main images); 100 µm (insets)). Representative images from ND- and HSD-fed mice ($n = 5$ per group). **e**, Thioflavin S staining is not present in mice fed an HSD, indicating absence of neurofibrillary tangles, which can be observed in rTg4510 mice (scale bars, 500 µm (main images); 100 µm (inset)). Representative images from $n = 5$ ND- and HSD-fed mice and $n = 3$ rTg4510 mice. **f**, HSD (4%) increases AT8 immunoreactivity in the neocortex but not in the hippocampus (AT8, cortex: ND/HSD $n = 5/5$, $^*P = 0.0148$ versus ND, two-tailed unpaired *t*-test). RZ3 was not increased in both regions. **g**, Time course of the increase in AT8 and RZ3 induced by HSD in the hippocampus. AT8 levels are increased after 4 weeks of HSD. RZ3 levels are increased after 4, 12, 24 and 36 weeks of HSD (AT8, 4 weeks: ND/HSD $n = 4/5$, $^*P = 0.0386$; 12 weeks: ND/HSD $n = 9/9$, $^*P < 0.0001$; RZ3, 4 weeks: ND/HSD $n = 4/5$, $^*P = 0.0041$; RZ3, 12 weeks: ND/HSD $n = 9/9$, $^*P = 0.0011$; 24 weeks: ND/HSD $n = 7/10$, $^*P = 0.0017$; 36 weeks: ND/HSD $n = 5/4$, $^*P = 0.0188$; two-tailed unpaired *t*-test for HSD versus ND). For gel source data see Supplementary Fig. 1. Data are expressed as mean ± s.e.m.

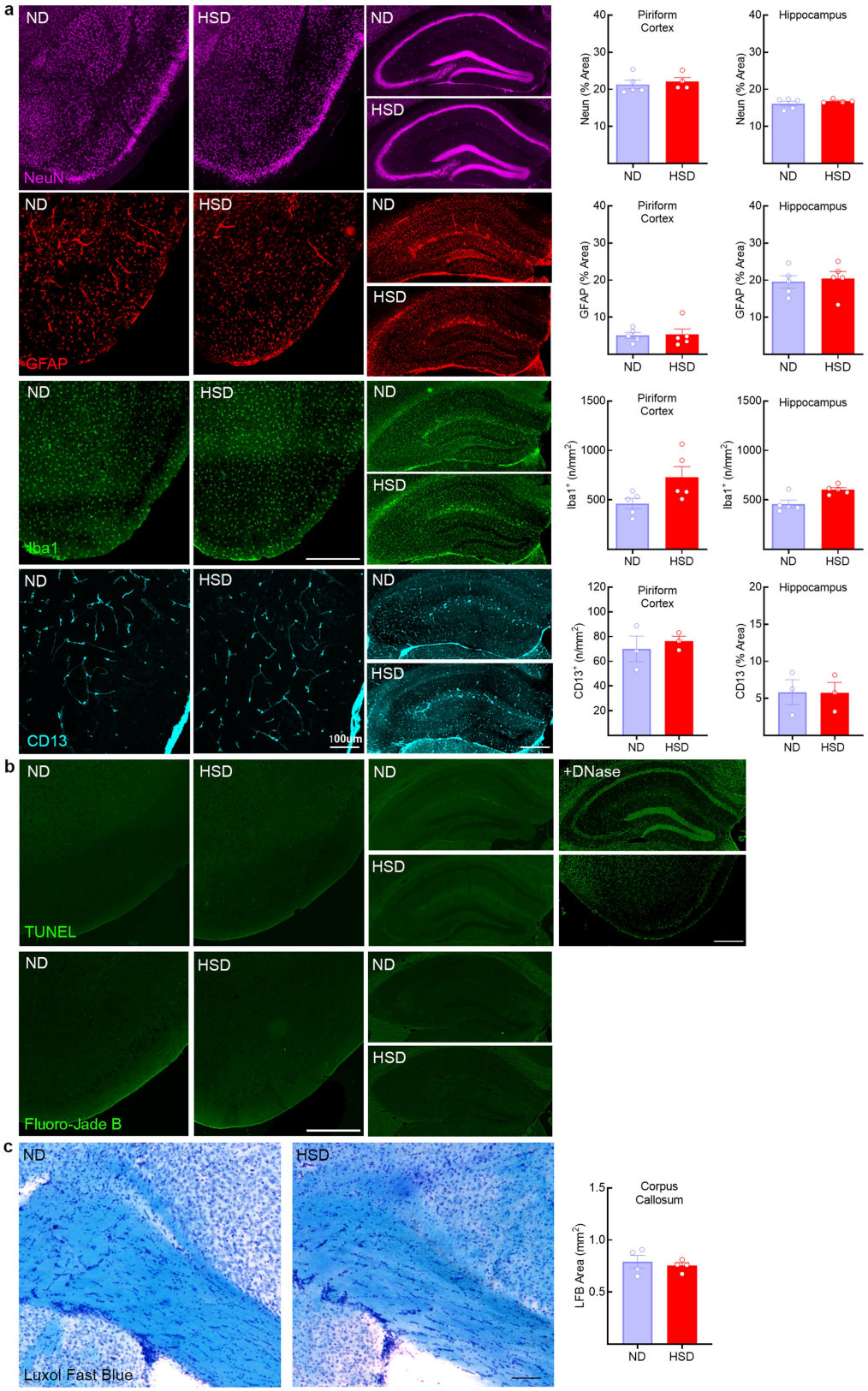

Extended Data Fig. 2 | Effect of HSD on neurons, astrocytes, microglia/macrophages, pericytes and white-matter integrity. a, HSD (NaCl 8%) does not affect neurons (NEUN), astrocytes (GFAP), microglia/macrophages (IBA-1) (cortex: microglia, ND/HSD $n = 5/5$, $P = 0.0570$; hippocampus: ND/HSD $n = 5/5$, $P = 0.0556$; two-tailed unpaired t-test for HSD versus ND) or pericytes (CD13) in both the pyriform cortex and the hippocampus (scale bars, 500 µm (except where specified)). **b**, No evidence of neuronal cell death is observed in HSD-fed mice by Fluoro-Jade B or TUNEL staining (scale bar, 500 µm). +DNase indicates positive control for TUNEL staining. Representative images from ND- and HSD-fed mice ($n = 5$ per group). **c**, Klüver–Barrera stain shows no white-matter damage in the corpus callosum of HSD-fed mice (scale bar, 100 µm). Representative images from ND- and HSD-fed mice ($n = 4$ per group). Data are expressed as mean ± s.e.m.

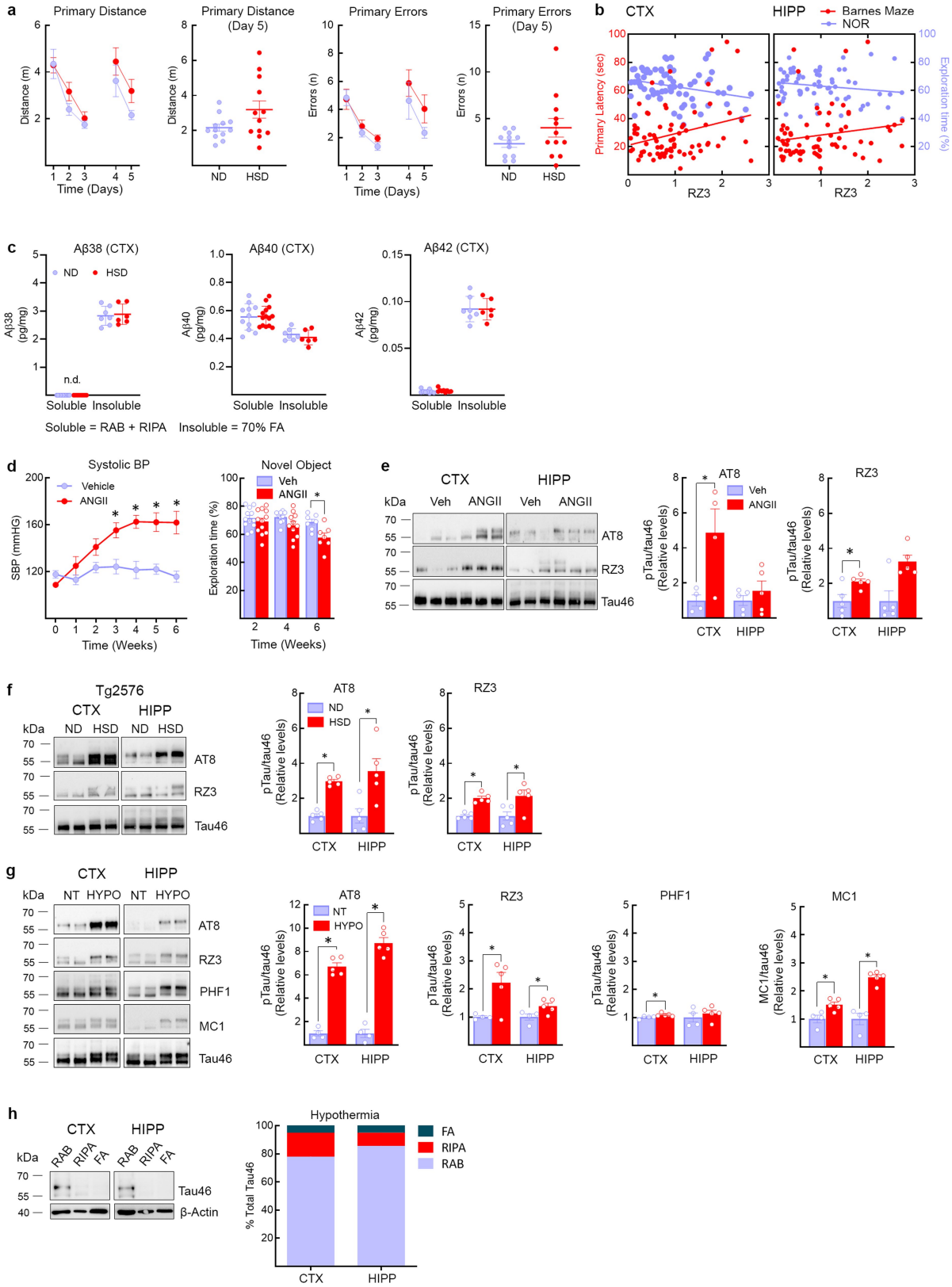

Extended Data Fig. 3 | See next page for caption.

Extended Data Fig. 3 | Aβ levels in HSD-fed mice and correlation of behavioural deficits with p-tau, as well as p-tau in hypertension, HSD-treated tg2576 mice and hypothermia. a, HSD (8% NaCl) does not alter the distance travelled before finding the escape hole in the Barnes maze (primary distance, ND/HSD $n = 13/13$, diet: $^*P = 0.0462$, time: $^*P < 0.0001$, two-way repeated measures ANOVA and Bonferroni's test; primary distance day 5: ND/HSD $n = 13/13$, $P = 0.0670$ versus ND, two-tailed unpaired *t*-test) or the number of errors made (primary errors, ND/HSD $n = 13/13$, diet: $P = 0.110$, time: $^*P = 0.0004$, two-way repeated measures ANOVA and Bonferroni's test; primary errors day 5: $P = 0.1226$ versus ND, two-tailed unpaired *t*-test). **b**, RZ3 levels in the cortex correlate with cognitive performance on the NOR test. No correlation was found between hippocampal RZ3 levels and cognitive performance on either the Barnes maze or the NOR test. RZ3 cortex: Barnes maze $r = 0.2828$, $^*P = 0.0133$, $n = 76$; NOR $r = -0.2806$, $^*P = 0.0170$, $n = 72$; RZ3 hippocampus: Barnes maze $r = 0.1739$, $P = 0.1470$, $n = 71$; NOR $r = -0.1746$, $P = 0.1577$, $n = 67$, Pearson's correlation coefficient). **c**, HSD does not increase soluble or insoluble $A\beta_{38}$, $A\beta_{40}$ or $A\beta_{42}$ in the neocortex. $A\beta_{38}$, soluble ND/HSD $n = 11/9$, insoluble ND/HSD $n = 7/6$; $A\beta_{40}$, soluble ND/HSD $n = 11/14$, insoluble ND/HSD $n = 7/6$; $A\beta_{42}$, soluble ND/HSD $n = 9/9$, insoluble ND/HSD $n = 7/6$. **d**, Delivery of angiotensin II (ANGII; 600 ng kg^{-1} min^{-1}, subcutaneously (s.c.)) via osmotic minipumps over 6 weeks increases systolic blood pressure (SBP) and induces cognitive deficits (SBP: Veh/ANGII $n = 10/10$, treatment: $^*P < 0.0001$, time: $^*P < 0.0001$, repeated measures two-way ANOVA and Bonferroni's test; NOR: 2 weeks Veh/ANGII $n = 12/12$, 4 weeks Veh/ANGII $n = 10/11$, 6 weeks Veh/ANGII $n = 7/7$, treatment: $^*P < 0.0021$, time: $^*P = 0.0208$, two-way ANOVA and Bonferroni's test). **e**, Administration of angiotensin II increases AT8 and RZ3 immunoreactivity in the neocortex but not the hippocampus (cortex, AT8 6 weeks: Veh/ANGII $n = 4/4$, $^*P = 0.0324$; RZ3 6 weeks: Veh/ANGII $n = 5/5$, $^*P = 0.0262$; hippocampus, AT8 6 weeks: Veh/ANGII $n = 5/5$, $P = 0.4056$; RZ3 6 weeks: Veh/ANGII $n = 5/5$, $P = 0.0556$, two-tailed unpaired *t*-test versus vehicle). **f**, HSD increases AT8 and RZ3 levels in both the neocortex and the hippocampus of 6-month-old Tg2576 mice (cortex, AT8: $^*P < 0.0001$; hippocampus, AT8: $^*P = 0.0153$; cortex, RZ3: $^*P < 0.0001$; hippocampus, RZ3: $^*P = 0.0239$; two-tailed unpaired *t*-test for HSD versus ND). **g**, Hypothermia induces massive AT8 phosphorylation (cortex: AT8 $n = 4/5$, $^*P = 0.0159$; hippocampus: AT8 $n = 4/5$, $^*P = 0.0159$) and increases MC1 (cortex: MC1 $n = 4/5$, $^*P = 0.0317$; hippocampus: MC1 $n = 4/5$, $^*P = 0.0159$) and RZ3 (cortex: RZ3 $n = 4/5$, $^*P = 0.0201$; hippocampus: RZ3 $n = 4/5$, $^*P = 0.0453$). Unpaired two-tailed *t*-test for hypothermia (HYPO) versus normal temperature (NT). **h**, Unlike HSD (Fig. 1G), hypothermia does not shift tau from soluble to more insoluble fractions. For gel source data see Supplementary Fig. 1. Data are expressed as mean ± s.e.m.

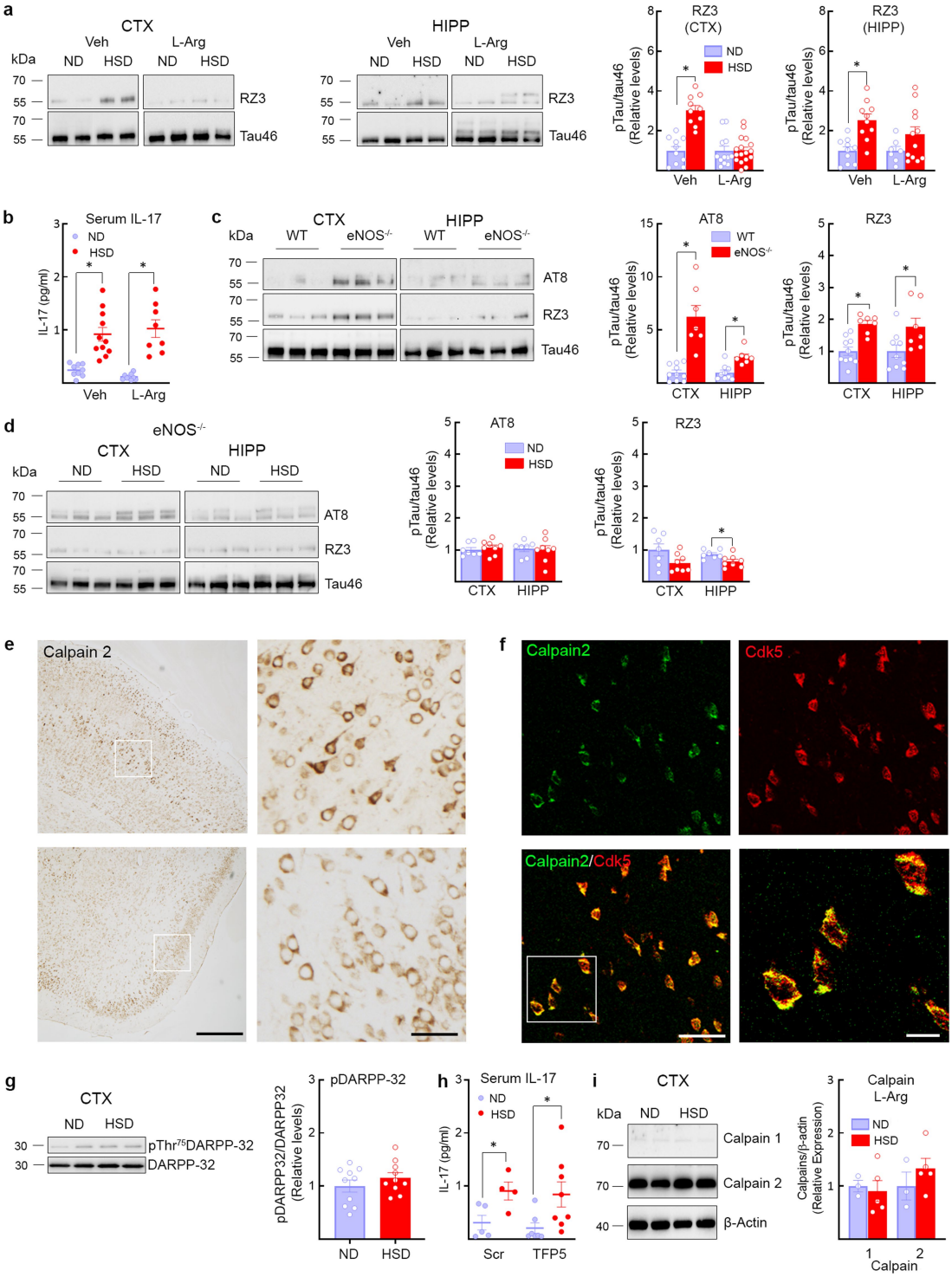

Extended Data Fig. 4 | Effect of L-arginine on p-tau and calpain expression, as well as p-tau in eNOS$^{-/-}$ mice, calpain and CDK5 localization, pDARPP-32 with HSD, and IL-17 levels. a, Administration of L-arginine (10 g l^{-1} in drinking water), starting at week 8 of HSD and continuing through week 12, suppresses RZ3 levels in the neocortex but not in the hippocampus (cortex: RZ3, ND/HSD $n = 10/10$, $^*P < 0.0001$; hippocampus: RZ3, ND/HSD $n = 10/10$, $^*P = 0.0005$, two-tailed unpaired *t*-test versus normal diet with vehicle). **b**, L-Arginine does not affect the increase in serum IL-17 induced by HSD (Veh, ND/HSD $n = 9/11$, $^*P = 0.0002$ versus ND Veh; L-arg, ND/HSD $n = 9/8$, $^*P < 0.0001$ versus ND L-arg, two-tailed unpaired *t*-test). **c**, AT8 and RZ3 levels are elevated in the neocortex and hippocampus of eNOS$^{-/-}$ mice on ND (AT8: cortex, ND/HSD $n = 5/4$, $^*P = 0.0029$; hippocampus, ND/HSD $n = 5/4$, $^*P = 0.0078$; RZ3: cortex, ND/HSD $n = 5/4$, $^*P = 0.0003$; hippocampus, ND/HSD $n = 5/4$, $^*P = 0.0128$, two-tailed unpaired *t*-test versus wild-type mice). **d**, HSD does not increase tau phosphorylation in eNOS$^{-/-}$ mice (RZ3: hippocampus, ND/HSD $n = 7/8$, $^*P = 0.0224$ versus ND, two-tailed unpaired *t*-test). **e**, Calpain 2 immunoreactivity is present in neuronal cell bodies of the somatosensory and piriform cortex (scale bars, 500 µm (left); 100 µm (right)). Representative images from $n = 3$ mice. **f**, Colocalization of Calpain 2 and CDK5 in neuronal cell bodies of the piriform cortex (scale bars, 50 µm (main images); 10 µm (inset)). Representative images from $n = 3$ mice. **g**, HSD has no effect on the phosphorylation of the CDK5 substrate DARPP-32 in neocortex; ND/HSD $n = 10/10$. **h**, Administration of the CDK5 peptide inhibitor TFP5 has no effect on the increase in serum IL-17 levels induced by HSD (scrambled: ND/HSD $n = 5/4$, $^*P = 0.0002$ versus ND scrambled; TFP5: ND/HSD $n = 7/8$, $^*P < 0.359$ versus ND TFP5; two-tailed unpaired *t*-test). **i**, L-Arginine does not alter the levels of calpain 1 and 2 in the neocortex or hippocampus. ND/HSD $n = 3/5$. For gel source data see Supplementary Fig. 1. Data are expressed as mean ± s.e.m.

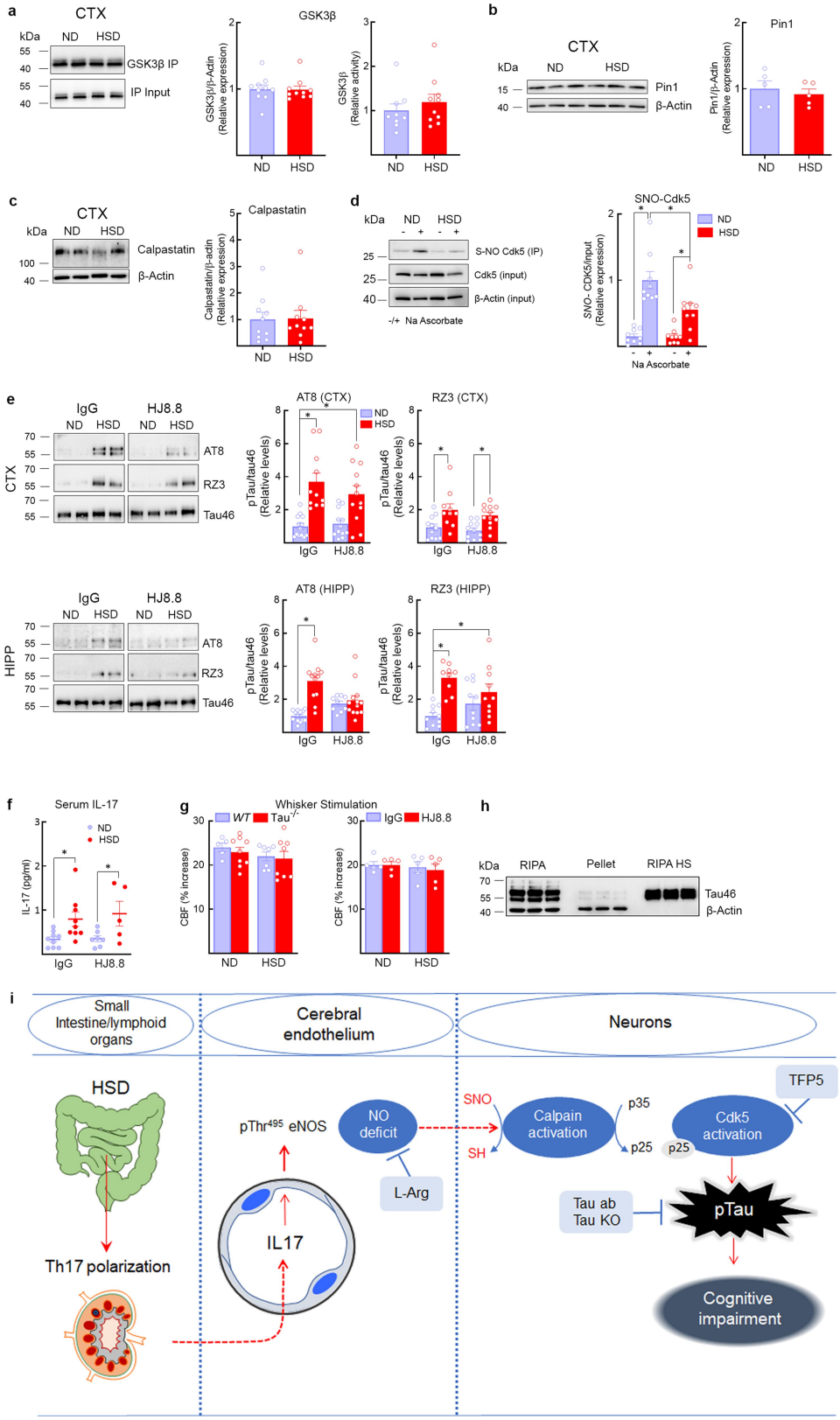

Extended Data Fig. 5 | See next page for caption.

Extended Data Fig. 5 | GSK3β, PIN-1, calpastatin and CDK5 nitrosylation in HSD-fed mice, as well as neurovascular coupling, effect of HJ8.8 on p-tau, serum IL-17, and summary. a, HSD has no effect on the expression or activity of GSK3β in the neocortex. ND/HSD $n = 10/10$. **b**, HSD does not alter the expression of the prolyl *cis/trans* isomerase PIN-1, a regulator of tau dephosphorylation. ND/HSD $n = 5/5$. **c**, The expression of calpastatin, an endogenous inhibitor of calpain activity, is not reduced by HSD. ND/HSD $n = 10/10$. **d**, Nitrosylation of CDK5 is reduced in the neocortex of HSD-fed mice (ND/HSD $n = 9/9$, diet: $^*P = 0.0143$; ascorbate: $^*P < 0.0001$; two-way ANOVA and Tukey's test). **e**, HJ8.8 reduces AT8 in the hippocampus (IgG: ND/HSD $n = 13/12$; HJ8.8: ND/HSD $n = 9/13$; $^*P < 0.0001$, Kruskal–Wallis test and Dunn's test). RZ3 levels are not altered by HJ8.8. **f**, Administration of HJ8.8 does alter the increase in serum IL-17 levels induced by HSD (IgG: ND/HSD $n = 9/9$, $^*P = 0.0192$ versus ND IgG; HJ8.8: ND/HSD $n = 7/5$, $^*P = 0.0421$ versus ND HJ8.8, two-tailed unpaired *t*-test). **g**, The increase in somatosensory cortex CBF induced by neural activity evoked by mechanical stimulation of the whiskers is not reduced by HSD in wild-type, tau$^{-/-}$ or HJ8.8-treated mice (wild-type ND/HSD $n = 5/7$, tau$^{-/-}$ ND/HSD $n = 9/8$; IgG ND/HSD $n = 5/5$, HJ8.8 ND/HSD $n = 5/5$). **h**, Western blotting showing enrichment of tau in boiled RIPA neocortical samples (heat-stable fraction, HS). Note that β-actin is lost during the boiling process. Representative images from $n = 3$ experiments. **i**, Cartoon depicting the mechanisms by which HSD leads to tau phosphorylation and cognitive impairment. HSD elicits a T_H17 response in the small intestine, which leads to an increase in circulating IL-17. IL-17, in turn, suppresses endothelial NO production by inducing inhibitory phosphorylation of eNOS at Thr495. The NO deficit results in reduced nitrosylation of calpain in neurons, and increases in calpain activity, p35 to p25 cleavage, activation of CDK5, and tau phosphorylation, which is ultimately responsible for cognitive dysfunction. In support of this chain of events, rescuing the endothelial NO deficit with L-arginine, lack of tau in tau-null mice, treatment with the CDK5 peptide inhibitor TFP5 or treatment with antibodies directed against tau (Tau ab) prevent the cognitive dysfunction. For gel source data see Supplementary Fig. 1. Data are expressed as mean ± s.e.m.

nature research

Corresponding author(s): Giuseppe Faraco, Costantino Iadecola

Reporting Summary

Nature Research wishes to improve the reproducibility of the work that we publish. This form provides structure for consistency and transparency in reporting. For further information on Nature Research policies, see Authors & Referees and the Editorial Policy Checklist.

Statistical parameters

When statistical analyses are reported, confirm that the following items are present in the relevant location (e.g. figure legend, table legend, main text, or Methods section).

n/a	Confirmed	
☐	☒	The exact sample size (*n*) for each experimental group/condition, given as a discrete number and unit of measurement
☐	☒	An indication of whether measurements were taken from distinct samples or whether the same sample was measured repeatedly
☐	☒	The statistical test(s) used AND whether they are one- or two-sided *Only common tests should be described solely by name; describe more complex techniques in the Methods section.*
☒	☐	A description of all covariates tested
☐	☒	A description of any assumptions or corrections, such as tests of normality and adjustment for multiple comparisons
☐	☒	A full description of the statistics including central tendency (e.g. means) or other basic estimates (e.g. regression coefficient) AND variation (e.g. standard deviation) or associated estimates of uncertainty (e.g. confidence intervals)
☐	☒	For null hypothesis testing, the test statistic (e.g. *F*, *t*, *r*) with confidence intervals, effect sizes, degrees of freedom and *P* value noted *Give P values as exact values whenever suitable.*
☒	☐	For Bayesian analysis, information on the choice of priors and Markov chain Monte Carlo settings
☒	☐	For hierarchical and complex designs, identification of the appropriate level for tests and full reporting of outcomes
☒	☐	Estimates of effect sizes (e.g. Cohen's *d*, Pearson's *r*), indicating how they were calculated
☐	☒	Clearly defined error bars *State explicitly what error bars represent (e.g. SD, SE, CI)*

Our web collection on statistics for biologists may be useful.

Software and code

Policy information about availability of computer code

Data collection	Chart 5 Pro (v5.5.6) was used for collection of CBF and MAP data. Any Maze (v5.3) was used for collection of behavioral data. IPLab-2.8.0 was used for acquiring phospho-Tau immunostaining images. Microsoft Excel (for Office365) was used for mouse randomization.
Data analysis	Chart 5 Pro (v5.5.6) was used for analysis of CBF data. Any Maze (v5.3) was used for analysis of behavioral data. Biorad Image Lab (v6.0) was used for analysis of immunoblots. Image J (v1.52p) was used for analysis of ASL MRI data. Graph Pad (v8.0) software was used for statistical analysis.

For manuscripts utilizing custom algorithms or software that are central to the research but not yet described in published literature, software must be made available to editors/reviewers upon request. We strongly encourage code deposition in a community repository (e.g. GitHub). See the Nature Research guidelines for submitting code & software for further information.

Data

Policy information about availability of data

All manuscripts must include a data availability statement. This statement should provide the following information, where applicable:

- Accession codes, unique identifiers, or web links for publicly available datasets
- A list of figures that have associated raw data
- A description of any restrictions on data availability

All data generated or analysed during this study are included in this published article (and its supplementary information files).

Field-specific reporting

Please select the best fit for your research. If you are not sure, read the appropriate sections before making your selection.

☒ Life sciences ☐ Behavioural & social sciences ☐ Ecological, evolutionary & environmental sciences

For a reference copy of the document with all sections, see nature.com/authors/policies/ReportingSummary-flat.pdf

Life sciences study design

All studies must disclose on these points even when the disclosure is negative.

Sample size	Sample size was determined according to power analysis based on previous published works published by our lab on CBF regulation and behavior.
Data exclusions	No data were excluded.
Replication	At least three independent experiments (with a number of subjects ranging from 3 to 5 each) were performed for all the findings in the manuscript. All attempts at replication were successful and are included in the figures.
Randomization	Mouse randomization was based on the random number generator function (RANDBETWEEN) in Microsoft Excel software.
Blinding	Analysis was performed in a blinded fashion.

Reporting for specific materials, systems and methods

Materials & experimental systems

n/a	Involved in the study
☒	☐ Unique biological materials
☐	☒ Antibodies
☒	☐ Eukaryotic cell lines
☒	☐ Palaeontology
☐	☒ Animals and other organisms
☒	☐ Human research participants

Methods

n/a	Involved in the study
☒	☐ ChIP-seq
☒	☐ Flow cytometry
☐	☒ MRI-based neuroimaging

Antibodies

Antibodies used

pTau Ser199Ser202, Rabbit polyclonal (ThermoFisher #44-768G); pTau Ser202Thr205 (AT8), Mouse monoclonal (ThermoFisher #MN1020); pTau Ser396 (PHF13), Mouse monoclonal (Cell Signaling #9632); pThr231 (RZ3) Mouse monoclonal (Gift from Prof. Peter Davies); MC-1 Mouse monoclonal (Gift from Prof. Peter Davies); K280, Rabbit polyclonal (Anaspec #AS-56077); pSer396 (PHF1), Mouse monoclonal (Gift from Prof. Peter Davies); Tau46, Mouse monoclonal (Cell Signaling #4019); p35/p25, Rabbit monoclonal, Clone C64B10 (Cell Signaling #2680); Cdk5, Rabbit polyclonal (Cell Signaling #2506); GSK3β, Rabbit polyclonal, Cell Signaling (#9315); Calpain 1, Rabbit polyclonal (Cell Signaling #2556); Calpain 2, Rabbit polyclonal (Cell Signaling #2539); Calpain 2 (IHC), Mouse monoclonal, E10 (Santa Cruz #373966); Calpastatin, Rabbit polyclonal (Cell Signaling #4146); pThr75 DARPP-32, Rabbit polyclonal (Cell Signaling #2301); DARPP-32 Rabbit polyclonal (Cell Signaling #2302); Pin1, Rabbit polyclonal (Cell Signaling #3722); β-Actin, Mouse monoclonal (Sigma #A5441); NeuN, Mouse monoclonal (Millipore #MAB377); Iba1, Rabbit ploYclonal (Wako #WEG2172); GFAP, Mouse monoclonal, clone G-A-5 (Sigma #63893); N/CD13, Goat polyclonal (R&D Systems #AF2335).

Validation	AT8 and pSer199Ser202 Tau antibody were validated by treating the brain samples with Lambda phosphatase. All phospho-Tau antibodies and the K280 antibody were also validated in mice with deletion of Tau. Cdk5 and p35p25 antibodies have been validated in immuno-precipitation experiments with IgG control antibody. All the other antibodies were extensively validated by us and/or in the literature.

Animals and other organisms

Policy information about studies involving animals; ARRIVE guidelines recommended for reporting animal research

Laboratory animals	Studies were conducted, according to the ARRIVE guidelines (https://www.nc3rs.org.uk/arrive-guidelines), in the following lines of male mice (age: 8weeks): C57BL/6 (JAX), B6.129X1-Mapttm1Hnd (Tau -/-, JAX, Stock #007251), Tg(Camk2a-tTA)1Mmay Fgf14Tg(tetO-MAPT*P301L)4510Kha/J (rTg4510, JAX, Stock#024854), B6.129P2-Nos3tm1Unc/J (eNOS-/-, JAX, Stock #002684), B6.129S4-Nos1tm1Plh/J (nNOS-/-, JAX, Stock #002986), and 129S6.Cg-Tg(APPSWE)2576Kha N20+? (Tg2576 or APPSWE, Taconic, Stock #279).
Wild animals	The study did not involve wild animals
Field-collected samples	The study did not involve field-collected samples.

Magnetic resonance imaging

Experimental design

Design type	*Indicate task or resting state; event-related or block design.*
Design specifications	*Specify the number of blocks, trials or experimental units per session and/or subject, and specify the length of each trial or block (if trials are blocked) and interval between trials.*
Behavioral performance measures	*State number and/or type of variables recorded (e.g. correct button press, response time) and what statistics were used to establish that the subjects were performing the task as expected (e.g. mean, range, and/or standard deviation across subjects).*

Acquisition

Imaging type(s)	Arterial Spin Labeling MRI
Field strength	7.0 Tesla 70/30 Bruker Biospec small-animal MRI system with 450 mT/m gradient amplitude and a 4500 T · m−1 · s−1 slew rate.
Sequence & imaging parameters	ASL-MRI was based on a flow-sensitive alternating inversion recovery rapid acquisition with relaxation enhancement (FAIR-RARE) pulse sequence labeling the inflowing blood by global inversion of the equilibrium magnetization.
Area of acquisition	The resting cerebral blood flow was measured in the cortex and in the hippocampus.

Diffusion MRI ☐ Used ☒ Not used

Preprocessing

Preprocessing software	*Provide detail on software version and revision number and on specific parameters (model/functions, brain extraction, segmentation, smoothing kernel size, etc.).*
Normalization	*If data were normalized/standardized, describe the approach(es): specify linear or non-linear and define image types used for transformation OR indicate that data were not normalized and explain rationale for lack of normalization.*
Normalization template	*Describe the template used for normalization/transformation, specifying subject space or group standardized space (e.g. original Talairach, MNI305, ICBM152) OR indicate that the data were not normalized.*
Noise and artifact removal	*Describe your procedure(s) for artifact and structured noise removal, specifying motion parameters, tissue signals and physiological signals (heart rate, respiration).*
Volume censoring	*Define your software and/or method and criteria for volume censoring, and state the extent of such censoring.*

Statistical modeling & inference

Model type and settings	*Specify type (mass univariate, multivariate, RSA, predictive, etc.) and describe essential details of the model at the first and second levels (e.g. fixed, random or mixed effects; drift or auto-correlation).*
Effect(s) tested	We tested the effect of high salt diet on the resting CBF. Specifically, we tested whether anti-tau antibodies restored the resting CBF reduction mediated by high salt diet.

Specify type of analysis: ☐ Whole brain ☒ ROI-based ☐ Both

Anatomical location(s) *Describe how anatomical locations were determined (e.g. specify whether automated labeling algorithms or probabilistic atlases were used).*

Statistic type for inference (See Eklund et al. 2016)

The images were analzyed by Image J and the average CBF value is reported as mL per 100g of tissue per minute.

Correction *Describe the type of correction and how it is obtained for multiple comparisons (e.g. FWE, FDR, permutation or Monte Carlo).*

Models & analysis

n/a	Involved in the study
☒	☐ Functional and/or effective connectivity
☒	☐ Graph analysis
☒	☐ Multivariate modeling or predictive analysis